UCSF
UC San Francisco Electronic Theses and Dissertations

Title

The regulation of somatostatin and parvalbumin inhibitory synapses onto hippocampal pyramidal neurons

Permalink

https://escholarship.org/uc/item/6q31g9vw

Author

Horn, Meryl Elizabeth

Publication Date

2017

Peer reviewed|Thesis/dissertation

eScholarship.org Powered by the California Digital Library
University of California

The regulation of somatostatin and parvalbumin inhibitory synapses onto hippocampal pyramidal neurons

by

Meryl Elizabeth Horn

DISSERTATION

Submitted in partial satisfaction of the requirements for the degree of

DOCTOR OF PHILOSOPHY

in

Neuroscience

in the

GRADUATE DIVISION

of the

UNIVERSITY OF CALIFORNIA, SAN FRANCISCO

for Jessica

Acknowledgements

I would first like to thank Roger Nicoll for his mentorship during my graduate school career. His sense of adventure in scientific discovery propelled my studies forward in such a way that I approached each new question from a place of curiosity and delight. He was generous in his encouragement and praise, and I could not have asked for a mentor more supportive of my scientific and professional development.

I would like to thank many members of the Nicoll laboratory, both past and present. I thank Kate Lovero, Adam Granger, Bruce Herring, John Gray and Maya Yamazaki for teaching me how to patch and troubleshoot problems with my rig when I first started. And I thank Nengyin Sheng, Salvatore Incontro, Javier Díaz-Alonso, Wucheng Tao, Jennifer Sun, and Michael Bemben, who helped guide my project forward as I continued on. I am especially grateful to Seth Shipman, who first introduced me to neuroligins and helped me establish an exciting and fulfilling rotation project, and to Jon Levy for his endless patience and kindness in helping me interpret my data. I would like to thank our wonderful laboratory technicians, Kirsten Bjorgan, Manuel Cerpas, and Dan Qin, whose friendship and support have vastly enhanced my time at the Nicoll lab. I am particularly grateful that my classmate and friend Samantha Ancona Esselmann happened to join the same lab as me, as her friendship and camaraderie helped my days pass quickly and joyfully. I would also like to thank the rest of my lunch crew, Joshua Emrick, Argentina Lario Lago, and Quynh-Anh Nguyen, who shared food, laughs and shade with me on countless occasions.

I would like to thank my committee members, Robert Edwards, Kevin Bender, Vikaas Sohal, and Massimo Scanziani, for sharing their expertise, helping me interpret my data and plan future experiments, as well as helping me strategize the publishing of my manuscript. It was

immeasurably valuable to receive their feedback, and after every committee meeting I returned to my experiments with a renewed sense of vigor and determination. I would also like to thank Vikaas Sohal for providing the PV-IRES-Cre and SOM-IRES-Cre mice, and Zachary Knight for providing the Ai32 mice, which were the basis of all experiments performed in this study.

Become a neuroscience graduate student after earning a college degree in an unrelated field depended on a series of unlikely events and the incredible support of several individuals. I would like to thank several professors at Hunter College: Robert Dottin, Roger Persell, and Shirley Raps. Without their advice and support it would not have been possible for me to begin a career in research. I thank my undergraduate mentor, Carmen Melendez-Vasquez, who had the willingness to take a chance on an eager student with no research experience. She entrusted me with the responsibility to guide my own project from an early point, an experience which gave me my first glimpse into the joy of scientific discovery.

I would like to thank my parents: Judith Stanley Horn and Laurence Horn, who raised me to appreciate the logic and the beauty of this world in equal parts. I thank my husband Christopher Suter, who boosted my spirits after days filled with long hours of patching, consoled me after defeats and celebrated victories with me during the past four years. I love you big time. I thank our cat, Oliver, and our dog, Penny, for providing snuggles and enthusiastic greetings when I come home. Finally, I thank Jessica Mack, my dear friend and roommate whom I lived with in New York City when I was first considering a career in science. It was she more than anyone else who encouraged me to continue on this path when my nascent scientific ambitions were most fragile.

Contributions

The collybistin real-time PCR experiment in Chapter 4, Fig. 1 was performed by Quynh Anh Nguyen when she was a graduate student in the Nicoll lab.

ABSTRACT OF THE DISSERTATION

The regulation of somatostatin and parvalbumin inhibitory synapses onto hippocampal pyramidal neurons

By Meryl Elizabeth Horn

Doctor of Philosophy in Neuroscience

University of California, San Francisco, 2017

Excitation/inhibition balance is critical for optimal brain function, yet the mechanisms underlying the tuning of inhibition from different populations of inhibitory neurons are unclear. Here, we found evidence for two distinct pathways through which excitatory neurons cell-autonomously modulate inhibitory synapses. Synapses from parvalbumin-expressing interneurons onto hippocampal pyramidal neurons are regulated by neuronal firing, signaling through L-type calcium channels. Synapses from somatostatin-expressing interneurons are regulated by NMDA receptors, signaling through R-type calcium channels. Thus, excitatory neurons can cell-autonomously regulate their inhibition onto different subcellular compartments through their input (glutamatergic signaling) and their output (firing). We found that in both the regulation of parvalbumin synapses by action potentials, and the regulation of somatostatin synapses by NMDA receptors represent alterations in the number of functional synapses.

Separately, little is known regarding whether synapses formed by somatostatin and parvalbumin interneurons onto pyramidal neurons are composed of different sets of post-synaptic components. Here, we found that while somatostatin and parvalbumin synapses onto excitatory neurons are both dependent on a common set of post-synaptic proteins, including gephyrin, collybistin, and neuroligin-2, somatostatin synapses are selectively impacted by neuroligin-3. Decreasing neuroligin-3 expression selectively decreases inhibition from

somatostatin interneurons, and overexpression of neuroligin-3 selectively enhances somatostatin inhibition. Together, these results provide evidence that excitatory neurons can selectively regulate two distinct sets of inhibitory synapses.

Table of Contents

CHAPTER 1 – General Introduction 1

Inhibitory Neuron Diversity...…….…….3

GABAergic Homeostasis ……..…5

Excitatory/Inhibitory Balance.…….……..……..……..7

The Molecular Composition of Inhibitory Synapses……...…….…….……..10

The Molecular Heterogeneity of Inhibitory Synapses……...…….…….……11

Rationale for the Approach Taken Here……...……..…….……13

CHAPTER 2 – Methods

Mouse transgenic lines …….……...…….....16

Experimental constructs…….…….……..…...16

Slice culture and biolistic transfection…….…….……...17

Electrophysiological Recording…….…….…….……18

Lentivirus production…….....…….…….....20

Real-time PCR…….……...……..……...……...20

Coefficient of variation analysis ……..…….……...……21

Statistical analysis....…….…….……...……....…...21

CHAPTER 3 – Differential homeostatic regulation of inhibitory synapses formed by PV vs. SOM-expressing interneurons

Introduction…….…….23

Results……..24

Synapses from PV-expressing inhibitory neurons are regulated by neuronal firing through L-type Calcium Channels…….....……...……...24

Synapses from SOM-expressing inhibitory neurons are regulated by NMDAR through R-type Calcium Channels…….……26

Discussion……...…….....……....28

CHAPTER 4 – Post-synaptic protein specialization at Parvalbumin vs. Somatostatin Inhibitory Synapses

Introduction……...……44

Results…….…….45

Gephyrin, Collybistin, and Neuroligin-2 regulate both PV and SOM-IPSC…….45

Neuroligin-3 selectively regulates SOM-IPSCs but not PV-IPSCs……...45

Discussion……..……..46

CHAPTER 5 – General Conclusions 59

The use of PV and SOM-Cre Mouse Lines: potential caveats ……...…....59

Is the "signal" spatial proximity, or intrinsic to the inhibitory synapse? ……60

Could NLGN3 be downstream of NMDAR dependent SOM-IPSC plasticity? …….……61

Comparison to other forms of NMDAR-dependent inhibitory plasticity……62

The composition of PV+ vs. SOM+ synapses……...……...…...63

The role of NLGN3 at SOM+ synapses……...……...……...….....64

Possibility of different secretory pathways for PV and SOM synapses……...….....65

The End Game: Just keep splitting?.....……...….....66

References **68**

List of Figures

CHAPTER 3

Figure 1 – Validation of ΔNav experimental construct. ……...……32

Figure 2 – PV-IPSCs are regulated by action potential firing through LTCC signaling. …...…..34

Figure 3 – The decrease in PV-IPSCs following Nav removal represents a decrease in the number of PV+ synapses……..……...……..36

Figure 4 – Effects of ΔGluN1 and GluN1 N616R on NMDAR currents …….……38

Figure 5 – Ablation of NMDA receptors selectively reduces SOM-IPSCs through RTCC signaling. ……..……...…….…….....40

Figure 6 – The decrease in SOM-IPSCs following NMDAR removal represents a decrease in the number of SOM+ synapses……...…….…….....42

CHAPTER 4

Figure 1 – Quantification of collybistin shRNA efficiency …….....…..49

Figure 2 – Reduction of gephyrin and collybistin affect both PV and SOM-IPSCs ……....51

Figure 3 - NLGN2 reduction affects both PV and SOM-IPSCs, while NLGN3 manipulations preferentially affect SOM-IPSCs ……..53

Figure 4 – The expression of NLGN3 on a NLGN2 miR background does not enhance NMDAR-mediated currents……...55

Figure 5 – Model summarizing results..…….……...57

CHAPTER 1

General Introduction

> "…it has been possible to establish that the synapses of different kinds are not mixed but rather grouped in special regions of the cell; some on the body, some on the origin of the dendrites, some on the end, etc., although, of course the fields of distribution of the synapses of different kinds often overlap."
>
> -Lorente de Nó, 1934, Studies of the structure of the cerebral cortex. II. Continuation of the study of the ammonic system.

Lorente de Nó was perhaps the first to recognize the potential functional importance of neuronal subtype diversity. A disciple of Santiago Ramón y Cajal, his attempt to reconstruct the microanatomy of neurons in the mouse cerebral cortex in 1933 provided the most complete accounting of neurological morphological diversity to date. He estimated that the mouse cortex "contains more than sixty perfectly defined types of nerve cells" (Fairén, 2007), which he referred to as "short-axon cells," now known as interneurons. He was also one of the first neuroscientists to recognize that different types of neurons generally showed different targeting properties. As the above quote illustrates, some types neurons targeted the body, some the dendrites. And remarkably, he correctly predicted that dendritic integration leads to a potential overcoming of a threshold. As he wrote in 1933, "The subliminal changes are summated first in

the dendrites and then in the surrounding of the axon. When the change reaches the threshold value, an explosive discharge through the axon takes place" (Fairén, 2007).

But Lorente de Nó is perhaps most known for formulating the current terminology for the subdivisions of the hippocampus. In "Studies on the structure of the cerebral cortex. Continuation of the study of the ammonic system" published in 1934, he postulated that the hippocampus be subdivided into the Cornu Ammonis (or "Ram's Horn") areas, which is now commonly abbreviated as CA1, CA2, and CA3. It was in this brain region that future neuroscientists would perform a heroic characterization of interneurons, cataloging their morphological and electrophysiological properties, lamellar distribution, genetic markers, and *in vivo* firing properties. Now, it is thought that there are closer to 15-20 subtypes of inhibitory neurons (Jiang et al., 2015; Klausberger and Somogyi, 2008), rather than the 60 de Nó observed.

Of course, it is now recognized that the vast majority of interneurons are inhibitory. While de Nó provided incredible insights into the anatomical diversity and functional importance of interneurons, at the time of his initial work, de Nó refused to accept the idea that inhibitory cells exist, as well as the fact that sodium was the ion responsible for the conduction of action potentials. Is it ever possible to realize which blind spots we possess, which prevent us from seeing the facts which will one day seem as equally obvious to us as the existence of inhibitory neurons?

The work in this thesis draws upon an array of literature composed of distinct threads. Besides inhibitory neuron diversity, a review of the current state of the fields of GABAergic homeostasis, excitatory/inhibitory balance, as well as the molecular composition and diversity of the inhibitory post-synaptic density will be necessary.

Inhibitory Neuron Diversity

Inhibitory neurons, that is, neurons which release the neurotransmitter the neurotransmitter γ-aminobutyric acid (GABA), only make up 10-20% of the total neuronal population in the hippocampus. However, they display a staggering amount of diversity. The most detailed cataloging of inhibitory neurons has been done in the hippocampus, likely because the simplicity of its lamellar structure lent itself easily to this endeavor. The main categories of inhibitory neurons in the hippocampus can be broadly categorized by their expression of genetic markers: parvalbumin-expressing (PV+), somatostatin-expressing (SOM+), cholecystokinin-expressing (CCK+), and 5HT3a Receptor-expressing (5HT3a+), all of which can be further broken down into more distinct subcategories.

The majority of CCK+ inhibitory neurons are "basket-cells," which refers to interneurons which target the soma of pyramidal neurons and whose cell bodies reside in the stratum pyramidale. One distinguishing feature of CCK+ interneurons is their expression of the CB1 cannabinoid receptors on their axonal terminals. These receptors mediate depolarization-induced suppression of inhibition, which is triggered by release of endocanabinoids from pyramidal neurons, acting in a retrograde manner (Wilson et al., 2001; Wilson and Nicoll, 2001). This was perhaps the first known case of pyramidal neurons selectively regulating inhibitory input from certain populations of interneurons. As a percentage of pyramidal neurons also express CCK, studying this population of inhibitory neurons, without also stimulating a small percentage of pyramidal neurons, has not been possible with the recent advances in optogenetically stimulation. 5HT3a+ cells have been more thoroughly characterized in the neocortex than the hippocampus. In the neocortex, they are comprised of two main categories:

cells also expressing the vasoactive intestinal peptide (VIP+) and neurogliaform cells (NGs) (Tremblay et al., 2016). VIP+ cells largely target other inhibitory neurons, especially SOM+ cells. NGs are thought to release GABA by volumetric transmission.

The two most widely characterized subtypes of inhibitory neurons, and the ones which will be subject of experimentation in this thesis, are PV+ and SOM+ cells. I will now focus on what is known about these two classes of inhibitory neurons in the CA1 region of the hippocampus. The majority of PV-expressing cells in CA1 are basket cells, which target the cell body and peri-somatic dendrites of pyramidal neurons. Other PV-expressing cells include axo-axonic cells, which target the axon-initial segment, and bistratified cells, which target the dendrites. PV+ interneurons make up an estimated 23.9% of the inhibitory neurons in the hippocampus. The basket cells and axo-axonic cells together account for 76% of this population, while bistratified cells account for the remaining 24% of PV+ cells (Bezaire and Soltesz, 2013). This indicates that the majority of PV+ cells in the hippocampus target the soma, peri-somatic region, or the axon-initial segment.

The largest groups of SOM+ cells are oriens-lacunosum moleculare (O-LM) cells, so-called because their bodies lie in stratum oriens, while their axons extend to stratum lacunosum moleculare. O-LM cells account for 40% of SOM+ cells in the hippocampus, the other 60% being composed of a diverse group of other inhibitory neurons, including double projection cells and oriens-retrohippocampal cells, which target both the dendrites of CA1 pyramidal neurons as well as the subiculum (Klausberger and Somogyi, 2008). It has also been documented that a proportion of bistratified neurons express both PV and SOM (Somogyi and Klausberger, 2005).

Therefore, while these populations of cells are not entirely non-overlapping in their targeting, it can be said that the majority of PV+ cells target the soma and the peri-somatic

region, whereas the majority of SOM+ cells target the dendrites. These overall targeting properties are found both in the hippocampus (Bezaire and Soltesz, 2013) and the neocortex (Tremblay et al., 2016), and are conserved in organotypic slices (Di Cristo et al., 2004).

Another interesting difference between SOM+ and PV+ cells in CA1 is the manner in which they get activated. Afferent fibers from CA3 stimulate both PV+ basket cells and CA1 pyramidal neurons in parallel, with PV+ basket cells then rapidly firing onto CA1 pyramidal neurons via disynaptic inhibition, in a microcircuit motif referred to as "feed-forward inhibition" (Hu et al., 2014; Pouille and Scanziani, 2001) (though there is also evidence that PV+ interneurons participate in other motifs, such as "lateral inhibition" (Hu et al., 2014)). SOM+ O-LM neurons are stimulated by local CA1 pyramidal neurons in stratum oriens, after which they may fire onto CA1 pyramidal neurons in stratum lacunosum moleculare, which is referred to as "feed-back inhibition" (Blasco-Ibáñez and Freund, 1995).

GABAergic homeostasis

The idea of synaptic homeostasis is that neurons will adjust their synaptic inputs in order to maintain a set level of firing (Turrigiano, 2011). It was first demonstrated to be true for excitatory inputs, in a landmark paper by Turrigiano et al. (Turrigiano et al., 1998), which showed that incubating a culture in tetrodotoxin (TTX), a toxin which blocks sodium channels and thus action potentials, causes an increase in miniature excitatory post-synaptic currents (mEPSCs). It was also shown that incubating a culture in bicuculline, which inhibits $GABA_AR$ and thus increases firing rate, causes a decrease in mEPSCs (Turrigiano et al., 1998). Together, this points to the idea that neurons will work to counteract changes in firing rates by adjusting their synaptic inputs.

It was not long before the Turrigiano lab also showed similar but opposing effects when examining miniature inhibitory post-synaptic currents (mIPSCs) (Rutherford et al., 1997). Incubating a culture in TTX causes a decrease in mIPSCs, while incubating a culture in bicuculline causes an increase in mIPSCs. This process was termed "GABAergic Homeostasis," and has since been shown to occur in multiple studies (Kilman et al., 2002; Peng et al., 2010; Pribiag et al., 2014; Saliba et al., 2007; Swanwick et al., 2006). Most of these studies find a change in both mIPSC amplitude and frequency, indicating that the size and number of inhibitory contacts are capable of being modulated.

Some studies gone on to investigate the possible molecular mechanisms that may underly the decrease in mIPSCs following TTX treatment. One study found that a decrease in brain derived neurotrophic factor (BDNF) may be required (Swanwick et al., 2006), while another study found that increased degradation of $GABA_AR$ in the endoplasmic reticulum-associated degradation pathway could be involved (Saliba et al., 2007). However, it is unclear from these experiments whether the phenomenon is cell-autonomous, as the TTX affects the entire network of neurons, including the excitatory and inhibitory cells. If one were to alter the firing rate of a single excitatory neuron, is this sufficient to cause a change in inhibitory inputs onto that cell?

The first study which attempted to do so failed to find evidence that cell-autonomous GABAergic homeostasis existed. Hartmen et al. (Hartman et al., 2006) used sparse transfection to either knock-down sodium channels or exogenously express an inwardly rectifying potassium channel, Kir2.1, which should lower the neuron's resting membrane potential and thus firing rate. In both of these experiments, the researchers failed to find any significant effects on mIPSCs. This suggests that the kind of GABAergic homeostasis that occurs following TTX or bicuculin treatment might indeed depend on a network-level action.

Since then, it is clear that there are conditions in which cell-autonomous changes in firing rate may alter inhibitory inputs onto that cell. In the Nicoll lab, Lu et al. (Lu et al., 2013) developed a mouse line which contained floxed GluA1,2,3, and GluN1 alleles. Combined with sparse infection with Cre, this leads to the elimination of all excitatory current from a small subset of pyramidal neurons in CA1. It was found that the electrically-induced IPSCs onto infected cells were decreased as compared to neighboring, uninfected control neurons. The authors also found that both mIPSC amplitude and frequency was decreased, though the decrease in mIPSC frequency was more pronounced. This suggests that there may be certain conditions in which cell-autonomous manipulations can lead to changes in the inhibitory input. It is possible that in the Hartmen et al. study, the manipulations still allowed for a low level of firing.

One clear limitation to these experiments is that it ignores the profound diversity of inhibitory neurons discussed earlier. When using mIPSCs or electrically-induced IPSCs, one cannot determine whether there are differences affecting only a subset of inhibitory inputs. It is now clear that PV+ neurons may be selectively affected by changes in firing rate (Bartley et al., 2008; Xue et al., 2014). However, before discussing those reports it is first necessary to explore another field relevant to this topic.

Excitatory/Inhibitory Balance

In parallel to the work examining homeostatic changes after *in vitro* pharmacological manipulations, the past two decades have also seen a growing recognition that excitatory and inhibitory brain activity is correlated *in vivo.* This has been found to hold true for both spontaneous and sensory-evoked activity, and is found in both the hippocampus and the neocortex (Atallah and Scanziani, 2009; Haider et al., 2006; Okun and Lampl, 2008; Wehr and

Zador, 2003; Wilent and Contreras, 2004). This phenomenon is referred to as "excitatory/inhibitory balance," and suggests that there are mechanisms at play to ensure that the total excitatory and inhibitory current amplitudes a neuron receives will correlate together over time (Eichler, 2008). It is thought that in order to maintain firing in a constant range, cells will adjust their inputs to ensure a constant ratio of excitatory and inhibitory inputs. It is recognized that this ratio may vary over development, and depend on the cell-type in question (Gao and Penzes, 2015).

To consider a concrete example, in the hippocampus *in vivo*, the amplitude of gamma rhythms will vary from cycle to cycle (Atallah & Scanziani 2009). The amplitude of inhibitory current varies in proportion to the amplitude of excitatory current, creating a stable excitation/inhibition ratio over time of about 1:4 (Atallah & Scanziani 2009). However, this phenomenon may be explained by the fact that more inhibitory neurons may be recruited as more schaffer collateral excitatory fibers are activated. At the time of this report, it was unclear whether individual neurons are also "hardwired" to receive proportionate levels of excitation and inhibition.

Xue et al., also from the Scanziani lab, went on to explore this new question in an elegant study published in 2014 (Xue et al., 2014). Using quadruple patching from acute slices in the visual cortex, Xue et al. here found that indeed, neurons are hardwired to receive proportional levels of excitatory and inhibitory currents. That is, the cells that received higher EPSC amplitudes upon ChR2 stimulation of excitatory fibers from layer 4 also received higher di-synaptic IPSCs amplitudes from the same fibers. They also found that pyramidal neurons that were firing at a higher rate *in vivo* (as measured by a Fos-EGFP mouse line) received higher IPSCs amplitudes. Of particular importance to the work shown here, the authors found cell-type

specific effects: IPSCs from PV+ inhibitory neurons onto pyramidal neurons (PV-IPSCs), but not IPSCs from SOM+ inhibitory neurons (SOM-IPSCs), showed stronger inhibition onto cells that were more active. Furthermore, PV-IPSCs were also responsive to artificially manipulating pyramidal cell activity in a cell-autonomous way. Decreasing firing by expressing a Kir2.1 channel caused a specific decrease in PV-IPSCs but not SOM-IPSCs, while increasing firing by expressing a bacterial sodium channel caused a specific increase in PV-IPSCs but not SOM-IPSCs. Thus, this study pointed to an activity-dependent regulation of inhibitory synapses formed by PV+ inhibitory neurons. This study corroborates earlier work done in organotypic slices from the somatosensory cortex, showing that slices incubated in TTX had reduced unitary-IPSC connections from PV+ inhibitory neurons, but not from SOM+ inhibitory neurons onto pyramidal neurons (Bartley et al., 2008).

These results lead to a model in which PV-IPSCs are uniquely responsive to changes in the target neuron's firing rate. Intriguingly, PV+ neurons are also poised to control the firing rate of pyramidal neurons, given the fact that the majority of PV-IPSCs target the soma and peri-somatic region, and axon initial segment, where action potentials are thought to be initiated.

So far, no circumstances have been found in which the inhibitory inputs of dendritic targeting inhibitory neurons or SOM+ neurons are specifically altered. However, one clue as to a possible mechanism comes from a follow-up study (Gu et al., 2016) from the lab of Wei Lu, the first author of the 2013 Nicoll lab paper showing that a cell-autonomous decrease in all excitatory current leads to a decrease in IPSCs (Lu et al., 2013). After reproducing the original result that elimination of both AMPAR receptors (AMPAR) and NMDA receptors (NMDAR) leads to a decrease in mIPSC frequency and amplitude, they examined the effects of just deleting AMPAR or NMDAR alone. Surprisingly, they found that only deletion of NMDAR, but not

AMPAR, was sufficient to decrease mIPSC frequency (Gu et al., 2016). This suggests that NMDARs might also play a role in the regulation of IPSCs. As NMDAR containing excitatory synapses are located on the dendrites, where SOM+ cells target, it is possible that it is SOM+ inputs which are particularly affected by alterations in NMDAR expression.

It is unclear why Lu et al. did not see a decrease in mIPSCs with the AMPAR deletion, as one would expect this to lower firing rate and potentially trigger a reduction in IPSCs as was found in Xue et al (Xue et al., 2014). However, it is possible that there are different "rules" governing the modulation of inhibitory inputs at the early time point at which the Lu et al. study was performed (using dissociated cultures taken from embryonic hippocampi and recording at 6 days *in vitro* (DIV)). Indeed, the authors describe this effect as a developmental requirement, rather than a homeostatic effect, given that under normal conditions, the effect of GABA release onto pyramidal neurons at this time point would be depolarizing (Gu et al., 2016).

The Molecular Composition of Inhibitory Synapses

As we dive deeper into the ways inhibitory synapses might be regulated, it becomes necessary to discuss the fundamental components of inhibitory synapses. Inhibitory synapses are composed of $GABA_A$ receptors ($GABA_AR$), as well as several $GABA_AR$ interacting proteins. $GABA_ARs$ are the GABA binding, heteropentameric, ion channels which are responsible for the majority of fast inhibitory transmission in the brain (Jacob et al., 2008). Several proteins have been shown to bind directly to $GABA_AR$ and regulate their trafficking. In particular, gephyrin is thought to be a powerful regulator of $GABA_AR$ and has been studied extensively. Gephyrin has been shown to stabilize $GABA_AR$ containing clusters at post-synaptic sites (Jacob et al., 2005) and to interact with cytoskeleton-binding proteins (Papadopoulos et al., 2007).

One protein thought to interact with gephyrin is collybistin, a guanine nucleotide exchange factor (GEF)-containing protein. Collybistin has been shown to alter the membrane targeting properties of gephyrin through its src homology 3 (SH3) region (Kins et al., 2000; Papadopoulos et al., 2007). Neuroligin-2 (NLGN2) is another gephyrin-interacting protein, a cellular adhesion molecule that binds to pre-synaptically expressed neurexin proteins (Südhof, 2017). NLGN2 is part of a larger family of NLGN proteins, including NLGN1, NLGN2, NLGN3, and NLGN4. Out of these isoforms, NLGN2 is the only family member which has been shown to be localized exclusively to inhibitory synapses (Varoqueaux et al., 2004). NLGN3 can localize to both excitatory and inhibitory synapses (Budreck and Scheiffele, 2007), while NLGN1 is thought to localize exclusively to excitatory synapses and the role of NLGN4 is unclear (Südhof, 2017).

Finally, dystroglycan and dystrophin are also thought to play a role in the stabilization of $GABA_AR$ at synapses. There are decreased clusters of $GABA_AR$ in mice lacking dystrophin (*mdx* mice, also a model of Duchenne muscular dystrophy) (Knuesel et al., 1999), and there is evidence that α-dystroglycan can regulate $GABA_ARs$ in an activity dependent manner (Pribiag et al., 2014). While gephyrin, collybistin, neuroligin-2, and dystroglycan are all thought to play a role in regulating the trafficking of $GABA_ARs$, inhibitory post-synaptic densities (iPSDs) are heterogeneous and show differing compositions of these proteins, as well as differing $GABA_AR$ subunits, at different synapses.

The Molecular Heterogeneity of Inhibitory Synapses

It has long been known that different iPSDs contain different $GABA_AR$ α subunits. Beginning in 2000, Thomson et al. (Thomson et al., 2000) showed that fast-spiking basket cells

(thought to be largely PV+) are more sensitive to zolpidem, a $GABA_AR$ α1 preferring agonist, compared to regular-spiking basket cells. This was corroborated by a study which showed that synapses from PV+ immunolabeled cells onto pyramidal neurons contain more $GABA_AR$ α1 than synapses formed by PV- cells (Klausberger et al., 2002). Conversely, regular spiking, somatically targeting PV- synapses contain a higher density of $GABA_AR$ α2 subunits, compared to PV+ synapses onto pyramidal neurons (Nyíri et al., 2001). While it was originally thought that these PV- synapses were likely CCK+, it was later shown that synapses formed by CCK+ inhibitory neurons likely contain a mixture of $GABA_AR$ α1, NLGN2, and dystrophin (Früh et al., 2016; Panzanelli et al., 2011). It is therefore unclear which subtypes of inhibitory input depend on the $GABA_AR$ α2 subunit.

It is clear from the gephyrin knock-out (KO) mouse that not all inhibitory synapses depend on gephyrin, as inhibitory transmission is largely intact: there is only a reduction in mIPSC amplitude by 23% while mIPSC frequency is unchanged in these animals (Lévi et al., 2004). However, it is unclear whether the gephyrin-independent synapses can be categorized in any meaningful way. According to one report using the gephyrin KO mouse, there is a loss of $GABA_AR$ α2, α3, β2/3, and γ2, while $GABA_AR$ α1 and α5 puncta remain (Kneussel et al., 2001). However, another report (Lévi et al., 2004) shows a subset of $GABA_AR$ α2, γ2 containing clusters which remain intact in the gephyrin KO mouse. Results from the $GABA_AR$ α2 KO mouse showed that multiple types of $GABA_AR$ α2 containing synapses may exist: a population of $GABA_AR$ α2, gephyrin, and NLGN2 containing synapses at the soma, as well as a population of $GABA_AR$ α2, α1, gephyrin and NLGN2 containing synapses at the axon-initial segment (Panzanelli et al., 2011). The collybistin KO mouse showed a loss of gephyrin puncta, with

evidence that dendritic inhibitory synapses were preferentially lost over somatic synapses (Papadopoulos et al., 2007).

There is also evidence that NLGN may show synapse-specific, as well as brain region-specific, roles. In dissociated hippocampal neurons taken from NLGN2 KO mice, there is a decrease in gephyrin puncta at the soma but not the dendrites, which mirrored a loss of gephyrin puncta in stratum pyramidale, but not stratum radiatum, in the hippocampus (Poulopoulos et al., 2009). Corroborating this, another study using the NLGN2 KO mouse, in the somatosensory cortex, found that unitary IPSCs evoked by PV+ cells, but not SOM+ cells, showed a decreased amplitude (Gibson et al., 2009). In the hippocampus of the NLGN3 knock-out mouse, unitary IPSCs evoked by PV+ cells remained unaltered, while unitary IPSCs evoked by CCK+ interneurons were increased (Földy et al., 2013). In the striatum, NLGN3 KO mice showed a reduction of mIPSC frequency onto medium spiny neurons expressing the dopamine receptor 1, but not 2 (Rothwell et al., 2014).

Together, this body of work indicates that there is certainly molecular heterogeneity among GABAergic synapses, both within neurons and between different brain regions. However, it is unclear which types of synapses correspond to which pre-synaptic inhibitory neuron subtypes.

Rationale for the Approach Taken Here

Much progress has been made in both characterizing the ways neurons can homeostatically alter their inhibitory input, and in determining the molecular composition of inhibitory synapses. However, these two fields seem to suffer from opposite problems: either too little granularity, or too much. In the field of GABAergic homeostasis, the vast majority of

studies have been limited to using the measurement of mIPSCs, from which nothing can be determined about whether the effects pertain to one or several classes of inhibitory neurons. Similarly, while several studies have shown that a balancing of excitatory and inhibitory currents exists *in vivo*, few studies (Xue et al., 2014) have investigated the cellular and molecular mechanisms underlying this effect. On the other hand, while several studies have determined the various combinations in which $GABA_AR$ subunits cluster with $GABA_AR$ trafficking proteins, no big picture has been resolved describing which types of inhibitory synapses depend on which proteins. The extent to which iPSDs formed by different subtypes of inhibitory neurons differ at the molecular level is largely unknown.

With the advent of optogenetic technology, it should be possible to make rapid progress in both of these fields. This is because it allows for the selective stimulation of genetically-defined subclasses of inhibitory neurons, without the need to use paired, unitary IPSC recordings. Here, I set out to accomplish two goals: (1) elucidate the molecular mechanisms of GABAergic homeostasis and (2) determine whether PV+ and SOM+ synapses depend on different sets of post-synaptic inhibitory proteins. I use PV-IRES-Cre mice and SOM-IRES-Cre mice, bred with Ai32 (lox-stop-lox-ChR2) mice, leading to expression of ChR2 selectively in either PV+ or SOM+ neurons. I then use biolistic transfection of organotypic, hippocampal slices to perform cell-autonomous manipulations on pyramidal neurons, and measure both PV+ mediated IPSCs (PV-IPSCs), and SOM+ mediated IPSCs (SOM-IPSCs) onto pyramidal neurons.

In Chapter 3, I explore the ways PV and SOM-IPSCs can be regulated in response to cell-autonomous manipulations of pyramidal neuron excitatory channel expression. I first confirm that PV-IPSCs can be regulated by firing in hippocampal organotypic slices, then discover a

novel form of homeostasis capable of regulating SOM-IPSCs. I also explore the molecular pathways through which these sets of synapses are regulated. In Chapter 4, I determine whether the canonical inhibitory proteins- gephyrin, collybistin, and NLGN2 and NLGN3- show differential effects on these sets of synapses. I find that there are both commonalities and differences in the proteins which PV+ and SOM+ synapses depend upon. Together, this work shows that pyramidal neurons are capable of regulating inhibitory input from PV+ vs. SOM+ neurons in distinct ways.

CHAPTER 2

Methods

Mouse transgenic lines

To express ChR2 in parvalbumin positive interneurons, PV-IRES-Cre mice (Jackson Laboratory Strain 008069) were bred with Ai32 mice, a Cre-dependent ChR2 line (Jackson Laboratory Strain 012569). To express ChR2 in somatostatin positive interneurons, SOM-IRES-Cre mice (Jackson Laboratory Strain 013044) were bred with Ai32 mice. Mice that were either heterozygous or homozygous for each gene were used for organotypic slice culture dissection. PV-IRES-Cre and SOM-IRES-Cre mice were a gift of Dr. V.S. Sohal, while Ai32 mice were a gift of Dr. Z.A. Knight. Animals were housed according to the IACUC guidelines at the University of California, San Francisco.

Experimental constructs

For CRISPR constructs, the following guide RNA (gRNA) targeting sequences were used (5' to 3'): Nav1.1, 1.2, and 1.3: TCCACTCCCCACACAGCACG; Nav1.6: GCTGCTGCAGAATGAGAAGA; GluN1 gRNA #1 AACCAGGCCAATAAGCGACA (validated in (Incontro et al., 2014)): GluN1 gRNA #2: AACCAGCCCACACCATGCCT (validated in (Straub et al., 2014)), GluN1 gRNA #3 ACTAGGATAGCGTAGACCTG (validated in (Incontro et al., 2014)). The gRNA sequences were ligated into pX458 to co-

express the human codon-optimized Cas9 as previously described (Incontro et al., 2014). To target sodium channels, we triple-coated gold particles with pX458 expressing gRNA targeting Nav1.1,1.2,1.3, pX458 expressing gRNA targeting Nav1.6, and pCAGGS-mCherry expressing plasmid in order to aid identification of transfected cells. To target GluN1, we co-coated the gold particles with either a pX458 plasmid expressing gRNA #1, gRNA #2, or gRNA#3, along with pCAGGS-mCherry. GluN1 N616R was mutated from the GluN1-1a splice variant and expressed in a pCAGGS expression plasmid (pCAG-GluN1 N616R-IRES-mCherry). Gephyrin miR targeting sequence was AACAGGGAATGAGCTACTAAA, validated in (Nguyen et al., 2016). Collybistin shRNA targeting sequence was AATCCGGAGAGACATCCTATA, validated in (Körber et al., 2012; Kuhse et al., 2012) and in Chapter 4, Fig. 1. NLGN2 miR targeting sequence was ATGGAGCAAGTTCAACAGCAA, validated in (Nguyen et al. 2016). NLGN3 miR targeting sequence was GCAGCGTTCTTGCAAGTTATG, validated in (Shipman and Nicoll, 2012). The NLGN3 overexpression construct was expressed in a pCAGGS expression construct containing IRES mCherry, and was based on human NLGN3 (accession number BC051715).

Slice culture and biolistic transfection

Hippocampal organotypic slice cultures were prepared from P6-P8 mice as described previously (Stoppini et al., 1991). All experiments were performed in accordance with established protocols approved by the University of California San Francisco Institutional Animal Care and Use Committee. Sparse biolistic transfections of organotypic slice cultures were performed as previously described (Schnell et al., 2002). Briefly, 50 μg each of plasmid DNA was coated on 1μm diameter gold particles in 0.5 mM spermidine, precipitated with 0.1 mM $CaCl_2$, and washed

four times in pure ethanol. The gold particles were coated onto PVC tubing, dried using ultra-pure N_2 gas, and stored at 4°C in desiccant. DNA-coated gold particles were delivered with a Helios Gene Gun (BioRad). Slices were maintained at 34 °C with media changes three times a week. All constructs were transfected on day 1 *in vitro*. Construct expression was confirmed by GFP and/or mCherry fluorescence. For the D-APV, MK-801, nifedipine, and SNX-482 experiments, slices were incubated in the drug from the time of transfection to the time of recording. SNX-482 was obtained from Peptides International, and bovine serum albumin (0.1 mg/mL) was added to the media to minimize nonspecific peptide binding.

Electrophysiological recording

Recordings were performed at 14-21 DIV. Dual whole-cell recordings in area CA1 were done by simultaneously recording responses from a fluorescent transfected neuron and a neighboring untransfected control neuron. IPSCs were recorded at 0 mV. For photostimulation, blue light was emitted from a Prizmatix UHP-LCC LED at 10 s interstimulus intervals. Intensity (0.05 mW-1 mW) and duration (~5ms) of light pulses were adjusted to produce reliable IPSCs of 100-1000 pA. We performed all recordings on an Olympus BX51WI microscope, using an Olympus ACROPLAN 63X/ 0.90 W objective.

NMDAR currents were evoked with a bipolar electrode placed in stratum radiutum and were measured at +40 mV in two different ways: (1) after the after wash-on of picrotoxin (0.1 mM) and bicuculline (0.01 mM), 150 ms after the stimulation, to ensure that any currents recorded were purely NMDAR-mediated, (2) or with the additional presence of NBQX (50 μM), measuring amplitude at the initial peak. 20 - 50 sweeps were averaged per pair. Typically each

pair of neurons is from a separate slice, whereas on rare occasions multiple pairs may come from one slice.

For all paired recordings, the number of experiments (n) reported in the figure legends refers to the number of pairs. CA1 pyramidal neurons were identified by morphology and location. Transfection under these conditions was sparse, and slices in which possible interneurons were also transfected in the same slice as a CA1 pyramidal neuron were thrown out. To ensure stable recording, membrane holding current, input resistance, and pipette series resistance were monitored throughout recording. All recordings were made at 20–25 °C using glass patch electrodes filled with an internal solution. Cesium-based internal solution was used for the majority of experiments, and consisted of 135 mM $CsMeSO_3$, 8 mM NaCl, 10 mM HEPES, 0.3 mM EGTA, 4 mM Mg-ATP, 0.3 mM Na-GTP, 5 mM QX-314, and 0.1 mM spermine. Potassium-based internal solution was used to validate the ΔNav construct, and consisted of 135 mM $KMeSO_4$, 10 mM NaCl, 2 mM $MgCl_2$, 1 mM EGTA, 10 mM HEPES, 14 mM phosphocreatine, 4 mM Mg-ATP, and 0.3 mM Na-GTP. External solution contained 119 mM NaCl, 2.5 mM KCl, 4 mM $MgSO_4$, 4 mM $CaCl_2$, 1 mM NaH_2PO_4, 26.2 mM $NaHCO_3$ and 11 mM glucose, and was bubbled continuously with 95% O_2 and 5% CO_2. For the ΔNav experiments, $KMeSO_4$-based internal was used to validate the construct, pulsing increasing amounts of current until the ΔNav cell either fired residual action potentials or failed to fire action potentials even with currents sufficient to elicit trains of action potentials in control cells (Chapter 3 Fig. 1). We initially recorded some PV-IPSCs and SOM-IPSCs using the $KMeSO_4$-based internal. After ensuring our ΔNav technique reliably eliminated or significantly reduced

action potentials, we switched to using a cesium-based internal. We found no difference between these conditions and therefore combined the data sets.

Paired-pulse ratios were examined using optogenetically evoked IPSCs at 50, 100, 200, 400, and 800 ms intervals. 6 stimuli were averaged per interval for each cell. Transfected and control neurons were recorded serially, adjusting the stimulus intensity for each neuron so that the first pulse produced IPSCs with approximately 200 pA peak amplitudes. Control neurons and transfected neurons were recorded from the same slice to control for inter-slice variation, moving to a new field of illumination in CA1 for the second recorded neuron, and varying whether the transfected or untransfected neuron was recorded from first. To measure the height of the second IPSC in cases where the first IPSC was overlapping with the second, we subtracted the contribution from the first IPSC, measuring from the point on the y-axis at which second IPSC began to its peak.

Lentivirus production

HEK293T cells were co-transfected with psPAX2, pVSV-G, and either NL2miR or Gephyrin-miR using FuGENE HD (Promega, Madison, WI). Supernatant was collected 40 hr later, filtered, and concentrated using PEG-it Virus Precipitation Solution (System Biosciences, Palo Alto, CA). Resulting pellet was resuspended in Opti-mem, flash-frozen, and stored at –80˚C.

Real-time PCR

Primary rat hippocampal dissociated neurons were prepared at E18.5 and infected with lentivirus expressing a collybistin shRNA or control GFP construct at DIV 4–7. Neurons were harvested at

DIV17-18 by lysis and reverse transcribed to synthesize cDNA using a Power SYBR Green Cells-to-CT kit (Life Technologies, Waltham, MA). Amplification of cDNA by real-time PCR was quantified using SYBR Green with the following primers: (fwd) TGCAAGAAGGACCTAATCCG, (rev) TCTCTT CTCTGAAAGCTCTAAGC.

Coefficient of variation analysis

Coefficient of variation (CV) analysis can be used to determine whether the locus of the decrease in PV and SOM-IPSCs is due to a change in quantal size (q), or quantal content (N x P_r). To perform this analysis, we calculated the CV^{-2}, defined as the (M^2/SD^2), where M is the mean IPSC amplitude and SD is the standard deviation for a set of successive sweeps. We calculated the CV^{-2} for the experimental and control cell, and plotted this ratio (CV^{-2}_{Expt}/ CV^{-2}_{Ctl}) against the ratio of mean amplitude (M_{Expt}/M_{Ctl}). Each of the grey circles in Chapter 3, Figures 3A and 6A represent a single pair of neurons. If these data points fall on the y = 1 line, the change in IPSC amplitude represents a change in quantal size, while if the data points fall on the identity line (grey dashed line), the change in IPSC amplitude represents a change in quantal content. This relies on the fact that changes in quantal size change both the mean IPSC and the variance such that the normalized ratio of CV^{-2} remains constant. In contrast, changes in quantal content will cause proportional changes of equal magnitude in CV^{-2}. Please see (Gray et al., 2011; Levy et al., 2015) for a more detailed description of this technique.

Statistical analysis

All paired whole-cell data were analyzed using a two-tailed Wilcoxon matched-pairs signed rank test. For comparisons of non-paired data including intrinsic excitability properties (Chapter 3

Fig. 1), paired-pulse ratios (Chapter 3, Figures 3B and 6B), and Chapter 3, Figure 4B, a Mann Whitney test was used. Outliers in IPSC data were removed using a ROUT test, Q = 5% on the $\log_{10}$ transfected/control data, on all paired IPSC data sets (3 out of 403 pairs were removed). For measuring rise time and action potential height, the start of the action potential was defined as the point at which the action potential reached 10% of its maximum slope. Data analysis was carried out in Igor Pro (Wavemetrics), GraphPad Prism (GraphPad Software) and Excel (Microsoft).

CHAPTER 3

Differential homeostatic regulation of inhibitory synapses formed by PV vs. SOM-expressing interneurons

Introduction

The majority of studies examining GABAergic homeostasis have been performed on dissociated neurons, using pharmacological manipulations that affect the entire network. A previous study from the Nicoll lab found that elimination of excitatory current in a pyramidal neuron causes a cell-autonomous decrease in IPSCs onto that neuron (Lu et al., 2013). Xue et al. (Xue et al., 2014) showed that although changes in pyramidal neuron firing in the visual cortex lead to positively correlated changes in IPSCs from PV+ interneurons onto those pyramidal neurons, pyramidal neuron firing does not change IPSCs from SOM+ interneurons. Additionally, elimination of NMDAR, but not AMPAR, in pyramidal neurons causes a decrease in IPSCs onto those cells (Gu et al., 2016), suggesting signaling through NMDARs is important for modulation of inhibitory inputs. While these studies indicate that excitatory neurons can alter their inhibitory inputs cell-autonomously, the mechanisms underlying this plasticity, and whether there are ways to specifically alter SOM synapses, are unclear.

Here, we confirmed the finding that PV-IPSCs are regulated by action potential firing, and discovered a new form of homeostatic plasticity wherein SOM-IPSCs are regulated by NMDAR. We found that these forms of homeostasis depended on different voltage gated

calcium channels, and both resulted in a reduction of quantal content, not quantal size. These results elucidate the ways in which pyramidal neurons can regulate different sets of inhibitory synapses.

Results

Synapses from PV-expressing inhibitory neurons are regulated by neuronal firing through L-type Calcium Channels.

We wanted to test whether there are different plasticity pathways selective for PV or SOM-IPSCs. As there is evidence that PV-IPSCs are regulated by the target neuron firing rate (Xue et al., 2014), we aimed to test this directly by using CRISPR/Cas9 to target pyramidal neuron sodium channels. Hippocampal pyramidal neurons express Nav1.2 and Nav1.6, and possibly trace amounts of Nav1.1 and Nav1.3 (Felts et al., 1997; Qiao et al., 2013). We therefore designed one guide RNA (gRNA) targeting Nav1.6, and one gRNA targeting a sequence present in Nav1.1, Nav1.2, and Nav1.3.

We first tested whether pyramidal neurons transfected with these gRNAs, along with Cas9 ("ΔNav"), were able to fire action potentials. We found that the majority (20/32) of transfected pyramidal neurons fired no action potentials (Fig. 1A). In the 12/32 pyramidal neurons that were still able to fire (Fig. 1B), we found that the action potentials had significantly slower rise times, decreased heights, and decreased slopes (Fig. 1C-E). Therefore, any action potentials remaining in ΔNav cells are likely of minimal strength.

In order to test whether the elimination of action potentials in pyramidal neurons would have an effect on PV-IPSCs, we crossed either PV-IRES-Cre or SOM-IRES-Cre mice with Ai32 (lox-stop-lox-ChR2) mice, leading to Cre-mediated excision of the floxed stop signal and

expression of ChR2 selectively in either PV or SOM neurons (PV:ChR2 or SOM:ChR2 mice) (Fig. 2A). We used PV:ChR2 and SOM:ChR2 mice for organotypic, hippocampal slice dissection at post-natal day 6-8. We used biolistic transfection of hippocampal slices at 1DIV, with the goal to selectively modulate pyramidal neuron gene expression, as this technique ensures very low transfection efficiency. IPSC recordings at 0 mV were made from pairs of transfected/untransfected CA1 pyramidal neurons between 2-3 weeks *in vitro*. We used PV:ChR2 mice to record light-evoked PV-IPSCs, and SOM:ChR2 mice to record SOM-IPSCs.

When we measured the PV-IPSCs, we found that they were significantly decreased in ΔNav cells (Fig. 2 B and E), while SOM-IPSCs showed no change (Fig. 3 C and E). These results support a model in which a cell-autonomous reduction of firing in pyramidal neurons causes a decrease in PV-IPSCs, but has no significant effects on SOM-IPSCs. These results confirm that we can replicate the results seen *in vivo* in the visual cortex (Xue et al., 2014), in hippocampal organotypic slices.

We then tested whether the mechanism through which neuronal firing regulates PV-IPSCs is dependent on L-type calcium channels (LTCC), as they have been found to mediate forms of action potential dependent excitatory homeostatic plasticity (Goold and Nicoll, 2010; Ibata et al., 2008; Levy et al., 2015; Thiagarajan et al., 2005). We incubated slices transfected with ΔNav in 20 μM nifedipine, a specific inhibitor of LTCC. As this will block LTCC on both the transfected and the control cells, any remaining difference between the cells indicates that the decrease in PV-IPSCs is not dependent on LTCC signaling. However, in the presence of nifedipine no difference in the size of PV-IPSCs was seen between ΔNav cells and control cells (Fig. 2 D and E), suggesting an occlusion of the effect. Therefore, elimination of action potential firing causes a decrease in PV-IPSCs through a reduction in current from LTCC.

Finally, we sought to determine whether the nature of the decrease in PV-IPSCs in ΔNav cells was due to a reduction in the number of functional synapses (N), a reduction in presynaptic release properties (P_r), or a reduction in the number of $GABA_A$Rs at each synapse (q). We decided to use coefficient of variation (CV) analysis, a technique which uses the inherent IPSC amplitude variability from trace to trace to differentiate between changes in quantal content ($N \times P_r$) and size (q) between two simultaneously recorded neurons (see Chapter 2, "Coefficient of variation analysis," for further description of this technique). As the data points fell along the dashed identity line, we found that the decrease in PV-IPSCs represents a change in quantal content ($N \times P_r$) rather than quantal size (q) (Fig. 3A). This indicates that the change in PV-IPSCs could either be due to a change in P_r or the number of functional synapses (N). To determine whether the decrease in PV-IPSCs in ΔNav cells is caused by altered P_r, we measured the paired-pulse ratio (PPR) of ΔNav and control cells. At no interval did we find a significant difference between the PPRs in ΔNav and control cells (Fig. 3B). Together, this indicates that the decrease in PV-IPSCs in ΔNav cells represents a change in N: an all-or-none loss in functional synaptic connections.

Synapses from SOM-expressing inhibitory neurons are regulated by NMDAR through R-type Calcium Channels.

We were next interested in studying the factors controlling SOM-IPSCs. Since alterations in NMDAR levels can regulate IPSCs (Gu et al., 2016), we decided to test whether NMDAR signaling might affect SOM-IPSCs, which largely target dendrites (Bezaire and Soltesz, 2013). We therefore used CRISPR/Cas9 to target the obligatory NMDAR subunit, GluN1 ("ΔGluN1"). We used one of two different gRNAs, both previously validated (Incontro et al., 2014; Straub et

al., 2014). We found robust reductions of NMDAR currents with both gRNAs (Fig. 4 A and B) and as expected, greater reductions in NMDAR current were observed with more days post-transfection (Fig. 4C), indicating that any residual current is due to slow NMDAR turnover. We found no significant differences in NMDAR-mediated current remaining between the gRNAs (Fig. 4B), so we combined the datasets. There was no change in PV-IPSCs in ΔGluN1 cells compared to control neurons (Fig. 5 A and H). However, we found a significant reduction in SOM-IPSCs in ΔGluN1 transfected pyramidal neurons. (Fig. 5 B and H).

To determine the mechanism through which NMDARs regulate SOM-IPSCs, we incubated slices in 200 μM D-APV, a competitive NMDAR antagonist which prevents glutamate binding to the NMDAR, and subsequent NMDAR activation-dependent depolarization of the neuron. Because the inhibitor will act on the control cells, we can use this experiment to determine whether the reduction in SOM-IPSCs in the ΔGluN1 cell is due to glutamate binding to the NMDAR. We found that this treatment occluded the decrease in SOM-IPSCs (Fig. 5 C and H), indicating a requirement for both glutamate binding to the NMDAR and presumably, the subsequent NMDAR- dependent depolarization.

Next, to determine explicitly whether ionotropic current through the NMDAR is necessary for this form of plasticity, we incubated slices in 100 μM MK-801, an NMDAR pore blocker. This, too also occluded the decrease in SOM-IPSCs in ΔGluN1 cells (Fig. 5 D and H). Finally, we attempted to rescue SOM-IPSCs by expressing GluN1 N616R, a mutant subunit impermeable to calcium (Sakurada et al., 1993). For these experiments we switched to "GluN1 gRNA #3," which targets an intron-exon junction of the *Grin1* gene so it would not target the rescue construct (Fig. 4D). We then co-expressed ΔGluN1 with GluN1 N616R. We confirmed the presence of GluN1 N616R by measuring NMDAR current at -70mV, as these channels are

insensitive to magnesium (Fig. 4E). Unexpectedly, this manipulation rescued the SOM-IPSCs (Fig. 5 E and H), indicating that calcium influx through NMDARs is unnecessary in regulating SOM-IPSCs. Instead, these results point to a model in which sodium influx through the NMDAR is necessary in the regulation of SOM-IPSCs.

In order to test whether other sources of calcium are required, we inhibited either LTCC or R-type calcium channels (RTCC), which are both found on spines (Davare et al., 2001; Yasuda et al., 2003). While incubation with 20 μM nifedipine did not block the relative decrease in SOM-IPSCs in ΔGluN1 transfected cells (Fig. 5 F and H), incubation with 500 nM SNX-482, an RTCC blocker, successfully occluded the decrease (Fig. 5 G and H). This suggests a pathway wherein NMDAR-driven sodium influx regulates SOM-IPSCs through RTCC.

We again used CV analysis on the SOM-IPSCs in ΔGluN1 cells, and found that this decrease also represents a change in quantal content, rather than quantal size (Fig. 6A). We also found no change in the PPR between the ΔGluN1 and control cells at any interval tested (Fig. 6B). Together, this suggests that similar to the decrease in PV-IPSCs in ΔNav cells, the decrease in SOM-IPSCs in ΔGluN1 cells represents an all-or-none loss in functional synaptic connections.

Discussion

Here, we show that the output of pyramidal neurons (action potential firing) regulates PV-IPSCs, while the input of pyramidal neurons (glutamatergic signaling via NMDARs) regulates SOM-IPSCs. This matches the known distribution of these inhibitory synapses: the majority of PV+ interneurons largely target the soma, peri-somatic dendrites, and axon initial segment of pyramidal neurons, while SOM+ interneurons target the more distal dendrites, which receive excitatory input (Bezaire and Soltesz, 2013). It has recently been estimated that

approximately 20% of spines contain inhibitory synapses (Villa et al., 2016). An intriguing possibility is that those SOM synapses co-localizing with excitatory synapses on spines are regulated by NMDARs.

We show that PV-IPSCs are regulated by action potential firing in a cell-autonomous manner. This agrees with what is known about the homeostatic regulation of IPSCs by neuronal firing in the neocortex, where it has been shown that pharmacological inactivation of firing with tetrodotoxin selectively reduces connection probability of unitary PV-IPSCs, while unitary SOM-IPSCs remain unchanged (Bartley et al., 2008), and *in vivo*, cell-autonomous alterations of firing rate in pyramidal neurons affects PV but not SOM-IPSCs onto those cells (Xue et al., 2014). We found that elimination of sodium channels does not reduce SOM-IPSCs (Fig. 2C), which suggests that local NMDAR-mediated spikes rather than back-propagating action potentials regulate these synapses. As main class of SOM+ interneurons are O-LM cells (Bezaire and Soltesz, 2013), they should target the distal dendrites in stratum lacunosum moleculare where it is likely that back-propagating action potentials play a relatively minor role in dendritic depolarization, compared to local excitatory synapses.

We have found that chronic removal of NMDARs leads to selective decreases in SOM-IPSC strength. Gu et al. (2016) showed that loss of NMDARs leads to a decrease in mIPSC frequency (Gu et al., 2016). Expressing a calcium impermeable NMDAR failed to rescue this effect, contrary to the mechanism reported here. One possible reason for this could be a lower level of RTCC expression in that study, which used dissociated hippocampal cultures at 6DIV from embryonic mice, compared to the present study, which uses organotypic slices at 17DIV from P6-8 mice. Indeed, dissociated hippocampal cultures from embryonic mice show far lower RTCC transcript levels compared to adult hippocampi (Schlick et al., 2010). The fact that in our

study, calcium entry through NMDAR is not sufficient to maintain the relative decrease in SOM-IPSCs following NMDAR removal (Fig. 5G) suggests that RTCC are uniquely positioned to initiate the downstream mechanisms needed to regulate SOM-IPSCs, potentially through calcium microdomains.

LTCC signaling has been shown to be required for multiple forms of excitatory synapse homeostasis, through CaMKK, CaMKIV, and transcriptional activation (Goold and Nicoll, 2010; Ibata et al., 2008; Levy et al., 2015). Potentially, PV-IPSCs are regulated by LTCC by similar transcriptional pathways. RTCC and LTCC also play a role in short-term plasticity of IPSCs in the visual cortex (Kurotani et al., 2008), by altering post-synaptic $GABA_AR$ expression through regulation of endocytosis and exocytosis. This suggests another possible downstream mechanism for the plasticity described here, though perhaps unlikely as the decreases in IPSCs here represent changes in quantal content.

We have found that both the decrease in PV-IPSCs in ΔNav cells and the decrease in SOM-IPSCs in ΔGluN1 cells represent changes in quantal content, rather than quantal size. This agrees with previous studies finding that eliminating AMPAR and NMDAR from pyramidal neurons causes mostly a decrease in mIPSC frequency rather than amplitude (Lu et al., 2013), and that eliminating NMDAR from pyramidal neurons causes only a decrease in mIPSC frequency but not amplitude (Gu et al., 2016). The decreases in PV-IPSCs and SOM-IPSCs described here may represent a decrease in the number of pre-synaptic release sites. Many studies have found roles for different mediators of retrograde signaling to inhibitory synapses, including BDNF (Peng et al., 2010), nitric oxide (Nugent et al., 2007) and endocannabinoids (Alger and Pitler, 1995). While endoccanabinoids are not likely to play a role, as CB1 receptors

are exclusively expressed on CCK+ cells, it is unclear whether other forms of retrograde signaling might play a role in the mechanisms described here.

Alternatively, the changes here may represent an all-or-none post-synaptic loss of $GABA_AR$, as the removal of post-synaptic proteins at excitatory synapses has been shown to cause all-or-none losses of glutamatergic receptors in an LTCC-dependent process (Levy et al., 2015). However, it is unknown whether there are specific post-synaptic proteins capable of altering PV vs. SOM-IPSCs inhibitory synapses in an all-or-none manner. While it would be difficult in our laboratory to determine which pre-synaptic mechanisms might be playing a role in the forms of plasticity described here, in the next chapter we set out to test whether several post-synaptically expressed proteins known to play a role in inhibitory transmission exert specific effects on PV vs. SOM-IPSCs.

Figure 1. Validation of ΔNav experimental construct.
(**A**) Sample traces showing control (black) and ΔNav transfected cell (green) with current pulses to elicit a single (left) and multiple (right) action potentials in the control cell. Transfected cell fired no action potentials, as in 20 of 32 cells. (**B**) Sample traces from neurons expressing ΔNav (green traces), or neighboring control neurons (black traces), showing a show typical transfected cell with residual action potentials (see arrows), as in 12 of 32 cells. (**C**-**E**) Summary plots show mean ± s.e.m on residual action potentials, showing increased rise time (C), decreased action potential height (D), and decreased maximum slope (E) as compared to control cell action potentials (n = 12 transfected cells, n = 23 control cells) ***$P < 0.001$.

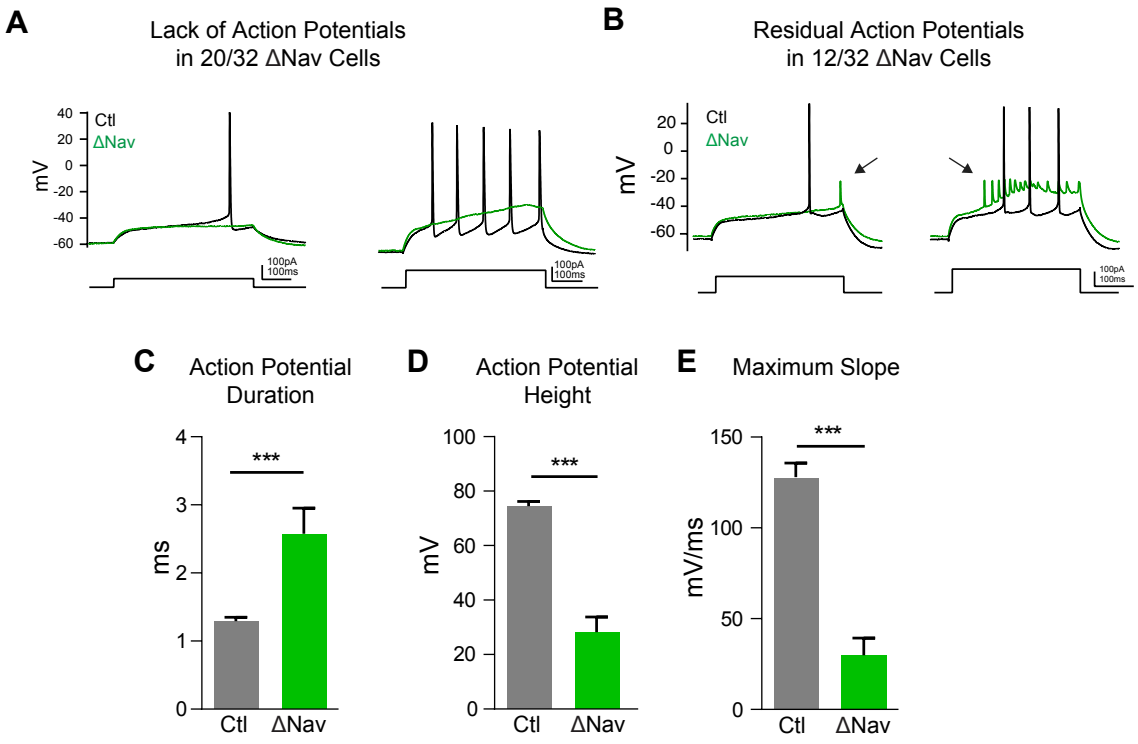
A
Lack of Action Potentials
in 20/32 ΔNav Cells
Ctl
ΔNav
mV
40
20
0
-20
-40
-60
100pA
100ms
B
Residual Action Potentials
in 12/32 ΔNav Cells
Ctl
ΔNav
mV
20
0
-20
-40
-60
100pA
100ms
C
Action Potential
Duration
ms
4
3
2
1
0
***
Ctl
ΔNav
D
Action Potential
Height
mV
100
80
60
40
20
0
***
Ctl
ΔNav
E
Maximum Slope
mV/ms
150
100
50
0
***
Ctl
ΔNav

Figure 2. PV-IPSCs are regulated by action potential firing through LTCC signaling. (**A**) Model showing mouse breeding scheme, experimental timelines, and patch-clamp configuration (**B**) Scatterplots show amplitudes of optically-evoked IPSCs recorded from pairs of ΔNav and control cells at approximately 17DIV in PV:ChR2 mice. (**C**) Same as in (B) but with SOM:ChR2 mice. (**D**) Same as in (B) but slices were incubated in 20 μM nifedipine from time of transfection to recording. (**E**) Summary plot showing IPSCs as a $\log_{10}$ of the ratio between transfected and control neurons, mean ± s.e.m. (PV-IPSCs, $P < 0.001$, $n = 27$; SOM-IPSCs, $P > 0.05$ $n = 27$, PV-IPSCs + nifedipine, $P > .05$, $n = 20$). Black sample traces are control, colored traces are transfected cells. Scale bars represent 200 pA and 40 ms ***$P < 0.001$.

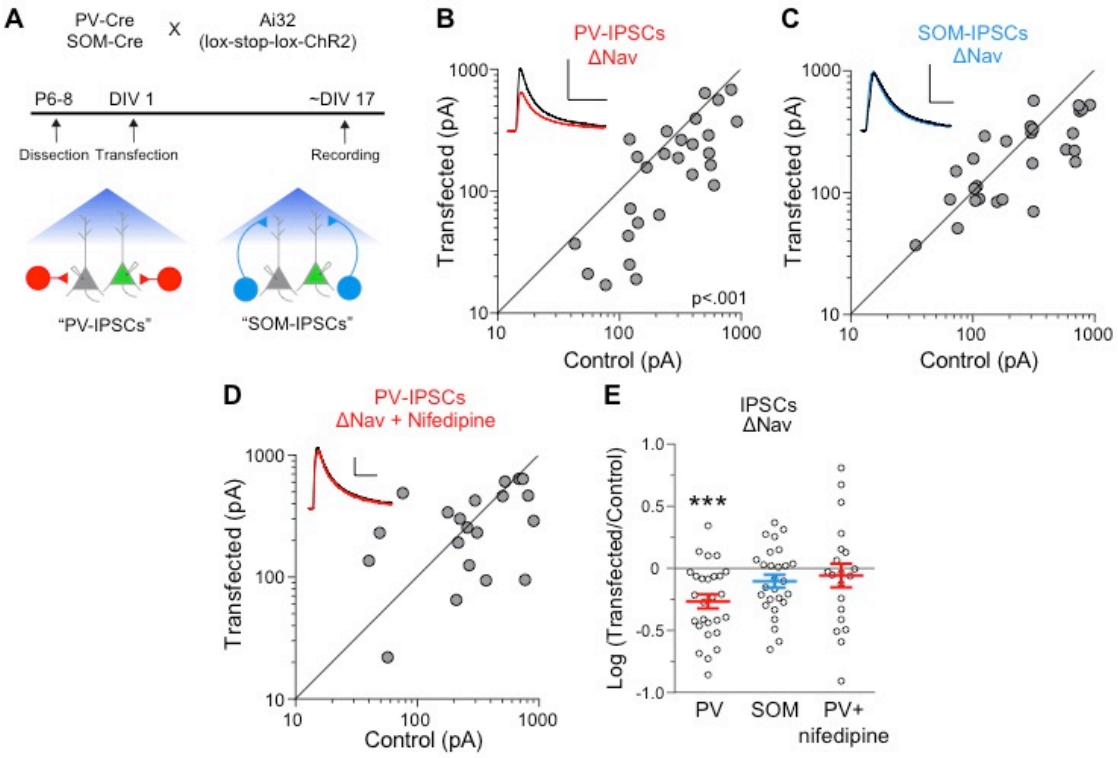
A
PV-Cre
SOM-Cre
X
Ai32
(lox-stop-lox-ChR2)
P6-8
DIV 1
~DIV 17
Dissection
Transfection
Recording
"PV-IPSCs"
"SOM-IPSCs"
B
PV-IPSCs
ΔNav
Transfected (pA)
Control (pA)
p<.001
C
SOM-IPSCs
ΔNav
Transfected (pA)
Control (pA)
D
PV-IPSCs
ΔNav + Nifedipine
Transfected (pA)
Control (pA)
E
IPSCs
ΔNav
Log (Transfected/Control)
***
PV
SOM
PV+
nifedipine

Figure 3. The decrease in PV-IPSCs following Nav removal represents a decrease in the number of PV+ synapses.

(**A**) Coefficient of variation analysis of simultaneously recorded pairs of control/ΔNav neurons. CV^{-2} graphed against ratio of mean amplitude within each pair. Results along the horizontal y = 1 line are consistent with change in quantal size (q), results along gray dashed identity (45°) line are consistent with change in quantal content ($N \times P_r$). Analysis of PV-IPSCs suggests decrease is due to reduction in quantal content. Small solid and dashed lines indicate linear regression line and 95% confidence intervals, respectively. (**B)** Paired-pulse ratios (PPR) of PV-IPSCs ($IPSC_2/IPSC_1$) recorded as a function of the interstimulus interval in ms. Summary plot shows mean PPR ± s.e.m for each interval, in ΔNav and control cells. To the right are representative traces of PV-IPSCs for both control (black) and ΔNav (red) cells, overlaid to show all intervals tested (50, 100, 200, 400, and 800 ms). Scale bars represent 100 pA and 150 ms. At no interval was there a statistically significant difference between the PPR in ΔNav and control cells. n = 9 transfected cells, n = 9 control cells.

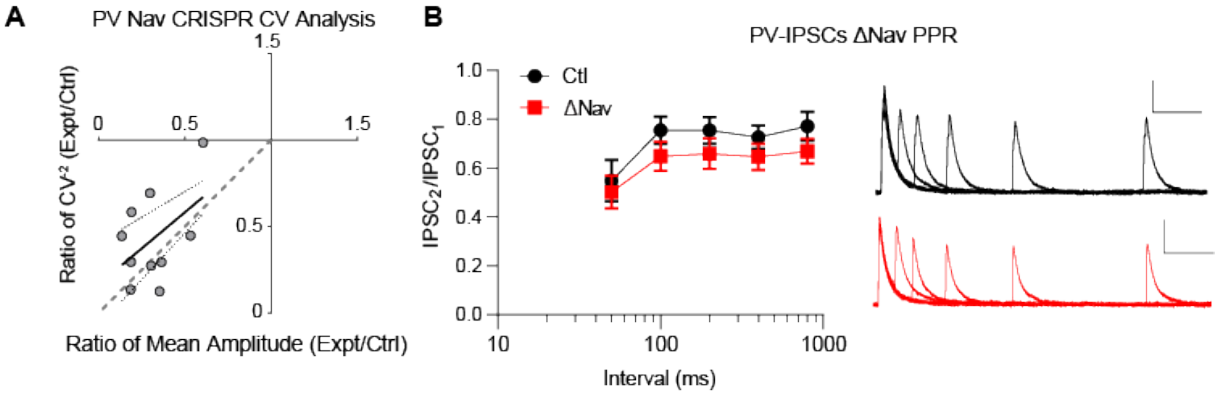
A
PV Nav CRISPR CV Analysis
1.5
0
0.5
1.5
0.5
0
Ratio of CV⁻² (Expt/Ctrl)
Ratio of Mean Amplitude (Expt/Ctrl)
B
PV-IPSCs ΔNav PPR
Ctl
ΔNav
1.0
0.8
0.6
0.4
0.2
0.0
IPSC2/IPSC1
10
100
1000
Interval (ms)

Figure 4. Effects of ΔGluN1 and GluN1 N616R on NMDAR currents.
(**A**) Paired data showing effects of GluN1 gRNA #1 and GluN1 gRNA #2 on NMDAR currents (gRNA #1, n = 13; gRNA #2, n = 18. (**B**) Summary plot showing NMDAR currents as a percent of control mean ± s.e.m. (**C**) Plot showing trend of further reductions of NMDAR currents with more days transfected. (**D**) Summary plot showing NMDAR currents remaining after transfection with intronic targeting GluN1 gRNA #3 (mean ± s.e.m., n = 10) (**E**) Paired data showing the effect of co-expressing ΔGluN1 (gRNA #3) with GluN1 N616R on NMDAR currents recorded at -70 mV ($P < 0.001$, n = 11). Black sample traces are control, colored traces are transfected cells. Scale bars represent 50 pA and 50 ms.

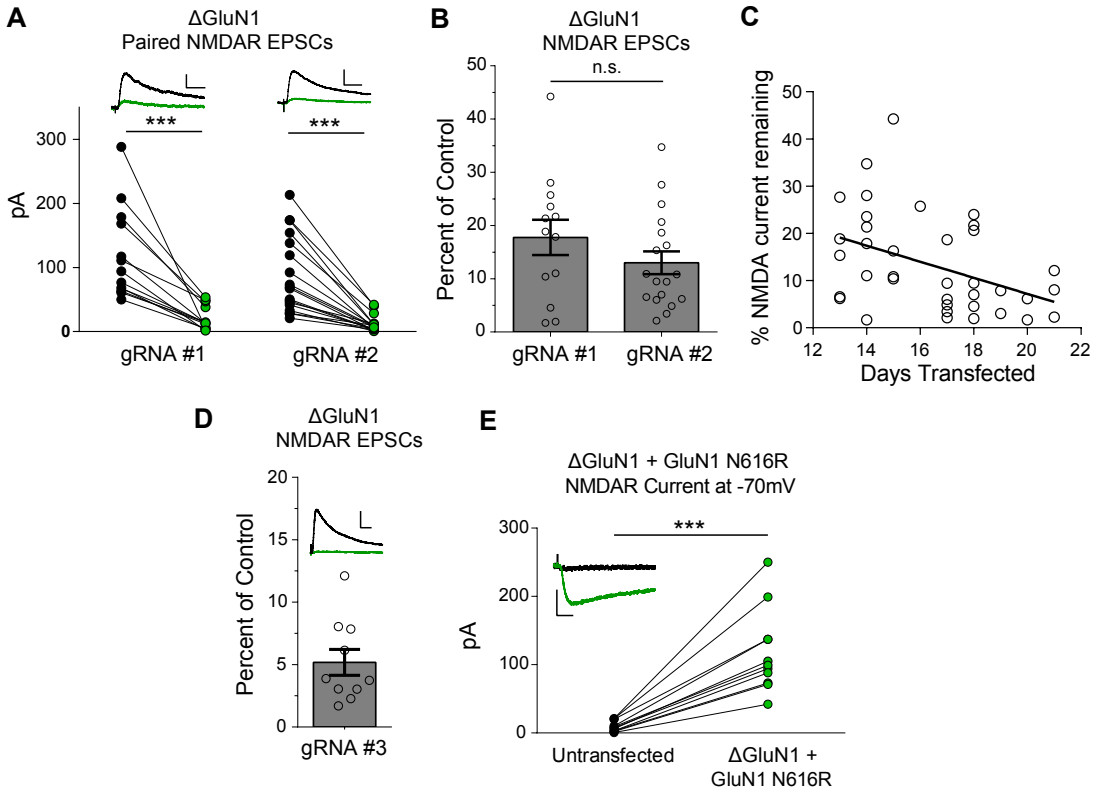
A
ΔGluN1
Paired NMDAR EPSCs
***
***
pA
300
200
100
0
gRNA #1
gRNA #2
B
ΔGluN1
NMDAR EPSCs
n.s.
Percent of Control
50
40
30
20
10
0
gRNA #1
gRNA #2
C
% NMDA current remaining
50
40
30
20
10
0
12
14
16
18
20
22
Days Transfected
D
ΔGluN1
NMDAR EPSCs
Percent of Control
20
15
10
5
0
gRNA #3
E
ΔGluN1 + GluN1 N616R
NMDAR Current at -70mV
***
pA
300
200
100
0
Untransfected
ΔGluN1 +
GluN1 N616R

Figure 5. Ablation of NMDA receptors selectively reduces SOM-IPSCs through RTCC signaling. (**A**) Scatterplots show amplitudes of IPSCs recorded from pairs of ΔGluN1 and control cells at approximately 17 DIV in PV:ChR2 mice. (**B**) Same as in (A) but with SOM:ChR2 mice. (**C**) Same as in (B) but incubating slices in 200 μM D-APV. (**D**) Same as in (B) but incubating slices in 100 μM MK-801. (**E**) Same as in (B) but expressing both ΔGluN1 and GluN1 N616R. (**F**) Same as in (B) but incubating slices in 20 μM nifedipine from time of transfection to recording. (**G**) Same as in (B) but incubating slices in 500nM SNX-482 from time of transfection to recording. (**H**) Summary plot showing IPSCs as a $\log_{10}$ of the ratio in transfected and control neurons, mean ± s.e.m. (PV-IPSCs $P > 0.05$, $n = 21$; SOM-IPSCs, $P < 0.001$, $n = 22$; SOM-IPSCs + APV $P > 0.05$, $n = 19$; SOM-IPSCs + MK-801 $P > 0.05$, $n = 20$; SOM-IPSCs + GluN1 616R $P > 0.05$, $n = 15$; SOM-IPSCs + nifedipine $P < 0.01$, $n = 20$; SOM-IPSCs + SNX-482, $P > 0.05$, $n = 18$). Black sample traces are control, colored traces are transfected cells. Scale bars represent 200 pA and 40 ms ***$P < 0.001$.

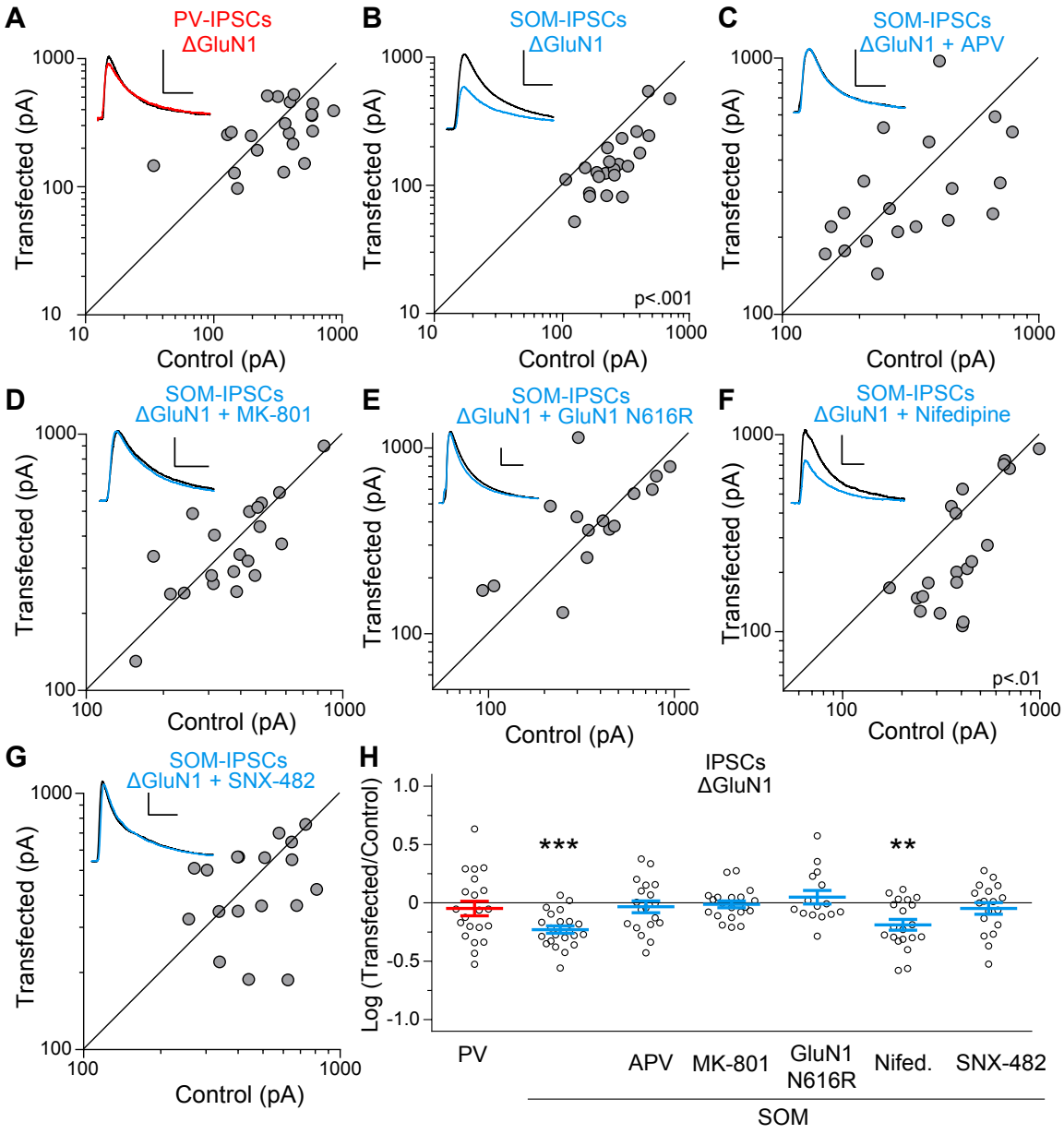
A
PV-IPSCs
ΔGluN1
B
SOM-IPSCs
ΔGluN1
p<.001
C
SOM-IPSCs
ΔGluN1 + APV
D
SOM-IPSCs
ΔGluN1 + MK-801
E
SOM-IPSCs
ΔGluN1 + GluN1 N616R
F
SOM-IPSCs
ΔGluN1 + Nifedipine
p<.01
G
SOM-IPSCs
ΔGluN1 + SNX-482
H
IPSCs
ΔGluN1
***
**
Log (Transfected/Control)
PV
APV
MK-801
GluN1 N616R
Nifed.
SNX-482
SOM
Transfected (pA)
Control (pA)

Figure 6. The decrease in SOM-IPSCs following NMDAR removal represents a decrease in the number of SOM+ synapses.
(**A**) Coefficient of variation analysis of simultaneously recorded pairs of control/ΔGluN1 neurons. CV^{-2} graphed against ratio of mean amplitude within each pair. Results along the horizontal y = 1 line are consistent with change in quantal size (q), results along gray dashed identity (45°) line are consistent with change in quantal content ($N \times P_r$). Analysis of SOM-IPSCs suggests decrease is due to reduction in quantal content. Small solid and dashed lines indicate linear regression line and 95% confidence intervals, respectively. (**B**) Paired-pulse ratios (PPR) of SOM-IPSCs ($IPSC_2/IPSC_1$) recorded as a function of the interstimulus interval in ms. Summary plot shows mean PPR ± s.e.m for each interval, in ΔGluN1 and control cells. To the right are representative traces of SOM-IPSCs for both control (black) and Δ GluN1 (blue) cells, overlaid to show all intervals tested (50, 100, 200, 400, and 800 ms). Scale bars represent 100 pA and 150 ms. At no interval was there a statistically significant difference between the PPR in ΔGluN1 and control cells. n = 8 transfected cells, n = 8 control cells.

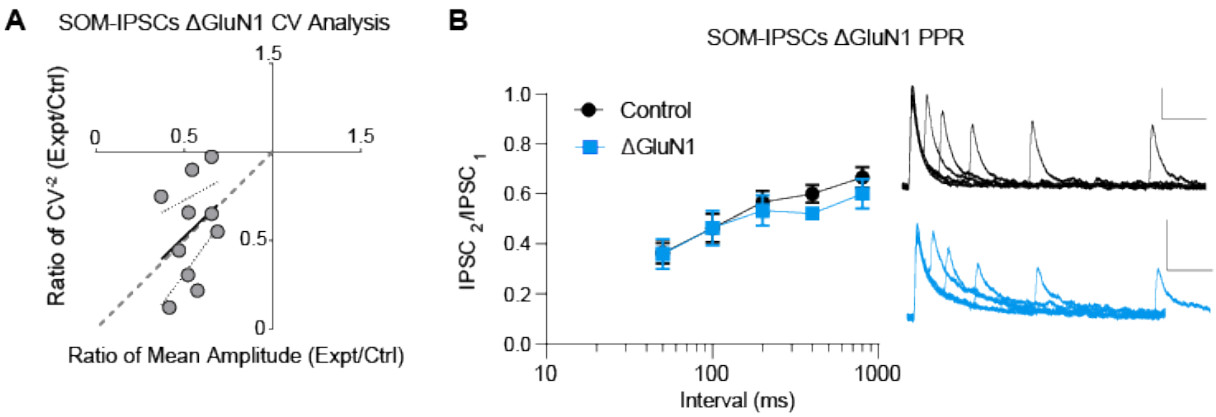
A
SOM-IPSCs ΔGluN1 CV Analysis
Ratio of CV-2 (Expt/Ctrl)
Ratio of Mean Amplitude (Expt/Ctrl)
0
0.5
1.5
B
SOM-IPSCs ΔGluN1 PPR
Control
ΔGluN1
IPSC 2/IPSC 1
Interval (ms)
10
100
1000
0.0
0.2
0.4
0.6
0.8
1.0

CHAPTER 4

Post-synaptic protein specialization at Parvalbumin vs. Somatostatin Inhibitory Synapses

Introduction

Recent studies have examined the composition of the inhibitory post-synaptic density in a high-throughput, non-biased manner (Kang et al., 2014; Uezu et al., 2016). However, from these studies it is impossible to determine whether this composition varies depending on the type of pre-synaptic inhibitory neuron forming the synapse. Indeed, it is unclear to what extent inhibitory synapses have different "types." Comparatively, there is a wealth of knowledge at the cellular and systems level which points to distinct inhibitory neuron subtypes displaying different physiological and morphological characteristics (Klausberger and Somogyi, 2008), and performing different roles at the behavioral level (Kepecs and Fishell, 2014).

While there is some evidence that neuroligin-2 is expressed at PV+ synapses (Gibson et al., 2009), and that dystrophin is expressed at CCK+ synapses (Früh et al., 2016), there is no evidence for a protein specifically expressed at inhibitory synapses contacting dendrites. Here, we tested whether several postsynaptic proteins expressed at inhibitory synapses showed specific effects on either synapses formed by either PV+ or SOM+ inhibitory neurons.

Results

Gephyrin, Collybistin, and Neuroligin-2 regulate both PV and SOM-IPSCs

To determine whether the canonical inhibitory post-synaptic proteins showed selective effects for PV vs. SOM-IPSCs, we used several validated (see Chapter 2, "Experimental constructs," Fig. 1) RNA-interference tools to test how reducing levels of gephyrin, collybistin, NLGN2 and NLGN3 impact PV and SOM-IPSCs. Transfecting pyramidal neurons with either a micro-RNA (miR) targeting gephyrin (Fig. 2 A, B and C), or a short hairpin RNA against collybistin (Fig. 2 D, E and F), both led to similar reductions in PV-IPSCs and SOM-IPSCs. We then tested NLGN2 and NLGN3, the two isoforms of neuroligins found at inhibitory synapses (Budreck and Scheiffele, 2007; Varoqueaux et al., 2004). We transfected pyramidal neurons with a miR targeting NLGN2, and found that both PV-IPSCs (Fig. 3 A and I) and SOM-IPSCs (Fig. 3 B and I) were dramatically decreased.

Neuroligin-3 selectively regulates SOM-IPSCs but not PV-IPSCs.

We then transfected pyramidal neurons with a miR targeting NLGN3. While transfecting pyramidal neurons with the NLGN3miR did not significantly affect PV-IPSCs (Fig. 3 C and I), SOM-IPSCs were decreased (Fig. 3 D and I). To verify the specificity of NLGN3 for SOM-IPSCs, we overexpressed NLGN3 in combination with NLGN2miR. This should prevent the dimerization of the overexpressed NLGN3 with endogenous NLGN2 (Budreck and Scheiffele, 2007; Shipman et al., 2011), and allow us to only look at the effects of NLGN3 homomers. We found that PV-IPSCs were reduced to a similar extent as the NLGN2miR on its own, suggesting that NLGN3 is not capable of enhancing these synapses (Fig. 3 E and I). However, overexpressing NLGN3 with NLGN2miR dramatically enhanced SOM-IPSCs (Fig. 3 F and I). We then tested whether overexpression of NLGN3 alone can enhance PV-IPSCs. This

manipulation still failed to enhance, and in fact led to a decrease in, PV-IPSCs (Fig. 3 G and I). As expected, NLGN3 overexpression profoundly enhanced SOM-IPSCs (Fig. 3 H and I). Together, these results show that while both PV-IPSCs and SOM-IPSCs depend on gephyrin, collybistin, and NLGN2, SOM-IPSCs are selectively and profoundly regulated by NLGN3.

It occurred to us that the increase of SOM-IPSCs following overexpression of NLGN3 might be due to an indirect effect of NLGN3 on NMDARs, as NLGN3 is known to localize to both inhibitory and excitatory synapses (Budreck and Scheiffele, 2007), and we have seen that NMDARs can regulate SOM-IPSCs (Chapter 3). However, NMDAR-mediated currents were not enhanced in NLGN3 + NLGN2miR cells (Fig. 4). Therefore, the effect of NLGN3 on SOM-IPSCs likely represents a direct effect at inhibitory synapses.

Discussion

These results provide evidence that synapses formed by PV and SOM-positive inhibitory neurons can be regulated in distinct ways (summarized with the results from Chapter 3 in Fig. 5). In the result which demonstrates this most clearly and dramatically, we show that while knocking down NLGN2 reduces both SOM and PV IPSCs to a similar extent (SOM: 29%, PV: 31%), overexpressing NLGN3 does nothing to enhance PV-IPSCs (they remain at 31%), while SOM-IPSCs are enhanced to 1124% of the control cell (Figure 3). This suggests that there are indeed different molecular compositions between synapses formed by PV+ and SOM+ cells.

We found that PV and SOM-IPSCs share a requirement for gephyrin, collybistin, and NLGN2. The fact that NLGN2 is required for SOM-IPSCs was surprising, given the fact that PV-unitary IPSCs but not SOM-unitary IPSCs are decreased in the NLGN2 KO mouse (Gibson et al., 2009). In that study, GIN (GFP-expressing Inhibitory Neurons) mice were used to identify

SOM neurons, and SOM-unitary IPSC recordings were made from layer 2/3 of the somatosensory cortex. It is therefore possible that there is a difference in the SOM cells being activated, or that cells have a differential dependence on NLGN2 depending on the brain region. Indeed, it has been demonstrated that NLGN3 exerts different effects on IPSCs depending on the cell-type and brain region being recorded from (Földy et al., 2013; Rothwell et al., 2014; Tabuchi et al., 2007). It is possible that NLGN2 also performs different roles depending on the type of pyramidal neuron being studied.

We find that reduction of NLGN3 selectively reduces SOM-IPSCs, and that overexpression of NLGN3 leads to a profound enhancement of SOM-IPSCs and a decrease of PV-IPSCs. It is possible that this decrease in PV-IPSCs is due to the fact that there is a limited amount of $GABA_A$ receptors ($GABA_AR$) in the pyramidal neuron, which are incapable of supporting the enhancement of SOM-IPSCs while maintaining normal levels of PV-IPSCs. Or, NLGN3 could be actively suppressing PV-IPSCs. In NLGN3 KO mice, PV-IPSCs onto hippocampal pyramidal neurons are unchanged, while CCK-IPSCs are increased (Földy et al., 2013). Together, this suggests that NLGN3 can have opposite effects on dendritic vs. somatic inhibition.

These results point to a model in which synapses formed by PV+ interneurons depend on gephyrin, collybistin, and NLGN2, while synapses formed by SOM+ interneurons depend on these proteins, as well as NLGN3. As overexpression of NLGN3 on a NLGN2 miR background was sufficient to enhance SOM-IPSCs, and reduction of NLGN3 reduced SOM-IPSCs, it suggests that NLGN3 homomers exist at synapses formed by SOM+ interneurons. However, the fact that using the NLGN2 miR reduced SOM-IPSCs to a dramatic extent (Fig. 3B), suggests that these NLGN3 homomers are not able to compensate for loss of NLGN2. This suggests that

while NLGN3 is capable of dramatically altering SOM-IPSCs, it may not be at SOM+ synapses in great abundance under baseline conditions.

The results in Fig. 4 show that NMDAR-mediated currents are not increased in cells in which NLGN3 is overexpressed on a NLGN2 miR background. This is an important control to ensure that NLGN3 is acting to directly enhance inhibitory synapses, as it is known that the overexpression of NLGN3 can affect excitatory currents in other conditions (Shipman et al., 2011). Another line of reasoning that support the role of NLGN3 affecting SOM+ synapses directly is that knockdown of NLGN3 with the miR decreases SOM-IPSCs, but we and others have found that elimination of NLGN3 does not decrease AMPAR or NMDAR mediated currents, either using a NL3 miR in adult CA1 pyramidal neurons (Shipman et al., 2011), or in single cell conditional deletion in dissociated hippocampal neurons (Chanda et al., 2017).

Together, these results show that it is possible to use optogenetic technology in combination with cell-autonomous manipulations to determine which post-synaptic inhibitory proteins exert effects at synapses formed by different subclasses of inhibitory neurons.

Figure 1. Quantification of collybistin shRNA efficiency.
Graph shows mean ± s.e.m. of collybistin mRNA remaining following treatment of dissociated hippocampal neurons with a virus expressing collybistin shRNA as assessed by real-time quantitative PCR, normalized to control GFP transduction (n = 2 technical replicates).

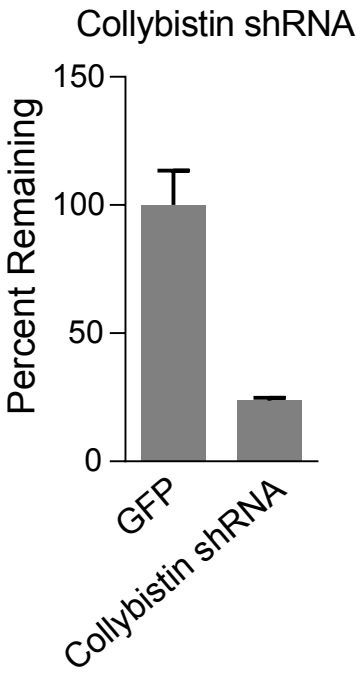
Collybistin shRNA
Percent Remaining
150
100
50
0
GFP
Collybistin shRNA

Figure 2. Reduction of gephyrin and collybistin affect both PV and SOM-IPSCs.
(**A**) Scatterplots show amplitudes of IPSCs recorded from pairs of gephyrin miR transfected and control cells at approximately 18 DIV (transfected ~2.5 weeks) in PV:ChR2 mice. (**B**) Same as in (A) but with SOM:ChR2 mice. (**C**) Summary plot showing IPSCs as a $\log_{10}$ of the ratio in gephyrin miR transfected and control neurons, mean ± s.e.m. (PV-IPSCs $P < 0.01$, $n = 16$; SOM-IPSCs, $P < 0.01$, $n = 18$). (**D**) Same as in (A) but transfecting with collybistin shRNA. (**E**) Same as in (**D**) but with SOM:ChR2 mice. (**F**) Summary plot showing IPSCs as a $\log_{10}$ of the ratio in transfected and control neurons, mean ± s.e.m. (PV-IPSCs $P < 0.001$, $n = 16$; SOM-IPSCs, $P < 0.001$, $n = 17$). Black sample traces are control, colored traces are transfected cells. Scale bars represent 200 pA and 40 ms. **$P < 0.01$ ***$P < 0.001$.

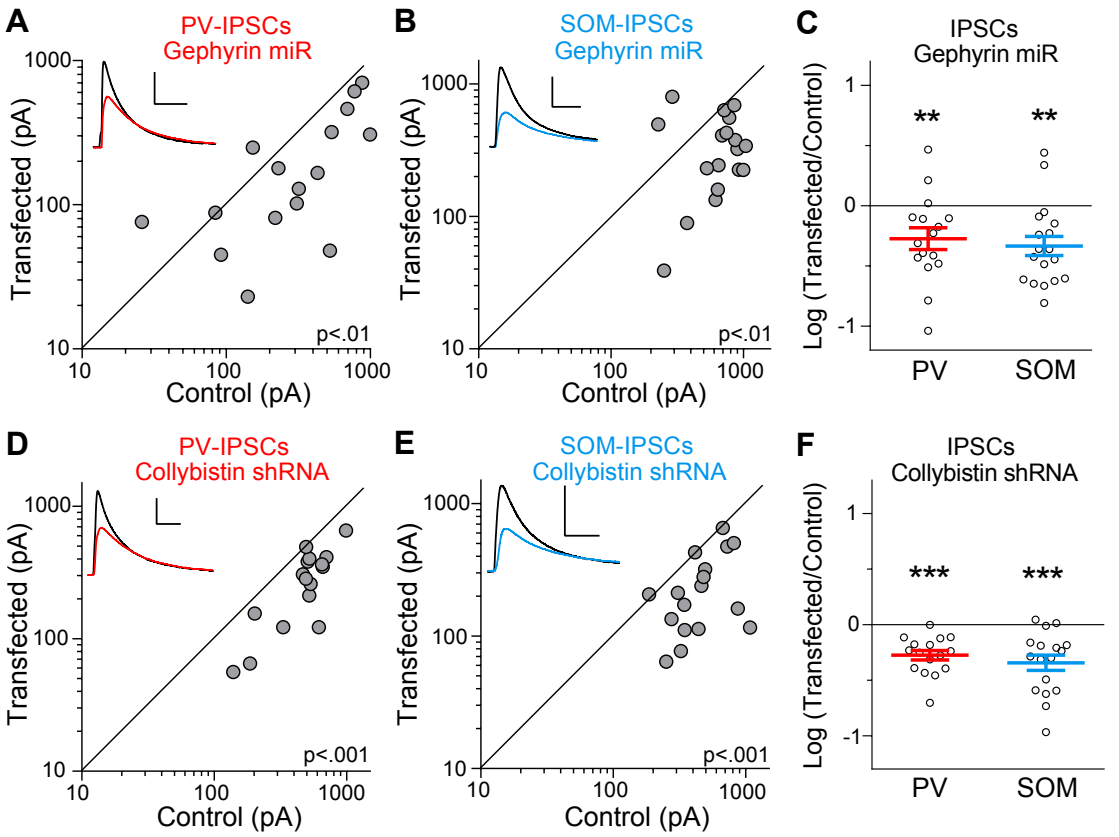
A
PV-IPSCs
Gephyrin miR
Transfected (pA)
Control (pA)
p<.01
B
SOM-IPSCs
Gephyrin miR
Transfected (pA)
Control (pA)
p<.01
C
IPSCs
Gephyrin miR
Log (Transfected/Control)
**
**
PV
SOM
D
PV-IPSCs
Collybistin shRNA
Transfected (pA)
Control (pA)
p<.001
E
SOM-IPSCs
Collybistin shRNA
Transfected (pA)
Control (pA)
p<.001
F
IPSCs
Collybistin shRNA
Log (Transfected/Control)
***
***
PV
SOM

Figure 3. NLGN2 reduction affects both PV and SOM-IPSCs, while NLGN3. manipulations preferentially affect SOM-IPSCs.
(**A**) Scatterplots show amplitudes of IPSCs recorded from pairs of NLGN2miR transfected and control cells at approximately 18DIV in PV:ChR2 mice. (**B**) Same as in (A) but in SOM:ChR2 mice. (**C**) Same as in (A) but transfecting with NLGN3miR. (**D**) Same as in (C) but in SOM:ChR2 mice. (**E**) Same as in (A) but expressing both NLGN2miR and overexpressing NLGN3. (**F**) Same as in E but in SOM:ChR2 mice. (**G**) Same as in (E) but only overexpressing NLGN3. (**H**) Same as in (G) but in SOM:ChR2 mice. (**I**) Summary plot showing IPSCs as a $\log_{10}$ of the ratio in transfected and control neurons, mean ± s.e.m. (NLGN2miR: PV-IPSCs $P < 0.001$, $n = 16$, SOM-IPSCs, $P < 0.001$, $n = 18$; NLGN3miR: PV-IPSCs $P > 0.05$, $n = 15$, SOM-IPSCs, $P < 0.05$, $n = 15$; NLGN2miR + NLGN3 o/e: PV-IPSCs $P < 0.001$, $n = 17$, SOM-IPSCs $P < 0.001$, $n = 17$; NLGN3 o/e: PV-IPSCs $P < 0.05$, $n = 15$, SOM-IPSCs $P < 0.001$, $n = 11$). Black sample traces are control, colored traces are transfected cells. Scale bars represent 200 pA and 40 ms. *$P < 0.05$ ***$P < 0.001$

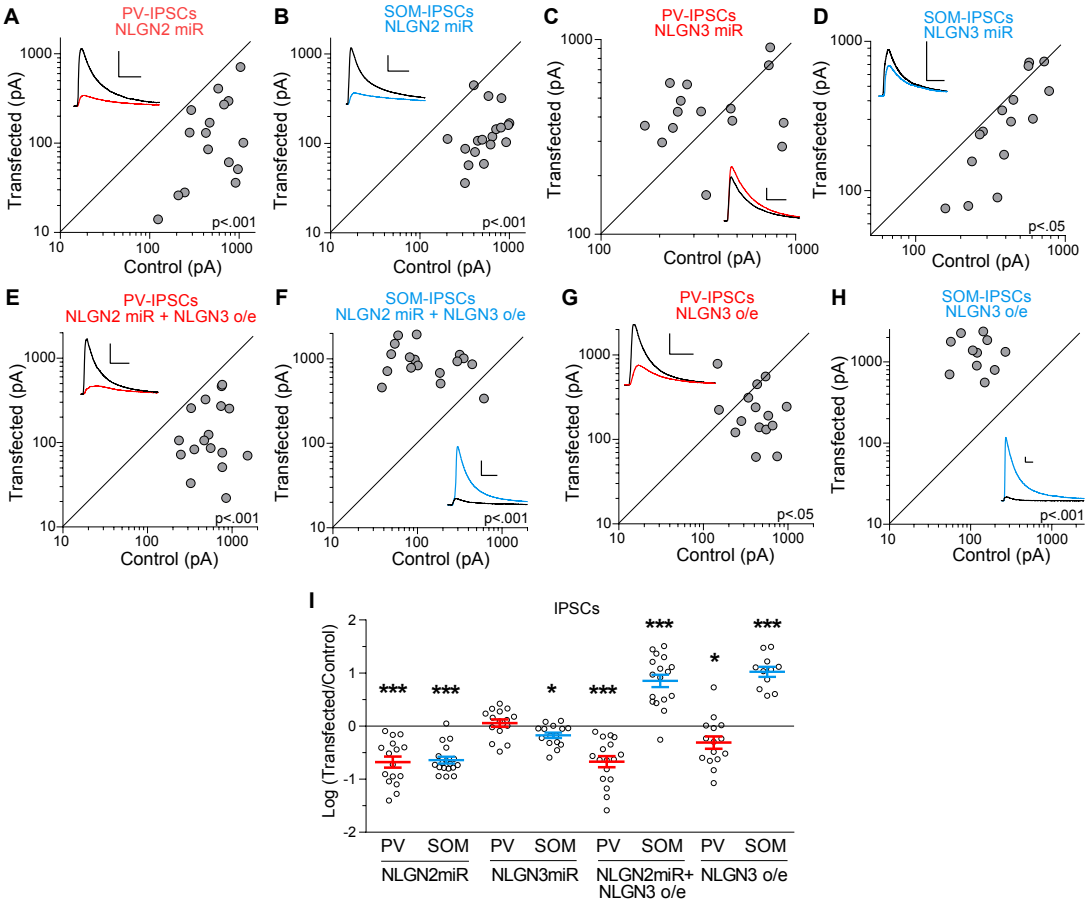
A
PV-IPSCs
NLGN2 miR
B
SOM-IPSCs
NLGN2 miR
C
PV-IPSCs
NLGN3 miR
D
SOM-IPSCs
NLGN3 miR
E
PV-IPSCs
NLGN2 miR + NLGN3 o/e
F
SOM-IPSCs
NLGN2 miR + NLGN3 o/e
G
PV-IPSCs
NLGN3 o/e
H
SOM-IPSCs
NLGN3 o/e
Transfected (pA)
Control (pA)
p<.001
p<.05
I
IPSCs
Log (Transfected/Control)
PV
SOM
NLGN2miR
NLGN3miR
NLGN2miR+
NLGN3 o/e
NLGN3 o/e

Figure 4. The expression of NLGN3 on a NLGN2 miR background does not enhance NMDAR-mediated currents.
Scatterplot shows amplitudes of electrically-evoked NMDAR-mediated current recorded from pairs of NLGN2miR + NLGN3 o/e transfected and control cells at approximately 18 DIV (transfected ~2.5 weeks) in PV:ChR2 mice, in the presence of bicuculin and picrotoxin, amplitude taken at 150 ms after stimulation (indicated by solid black line in sample trace) to eliminate contribution from AMPAR-mediated currents. Summary plot showing IPSCs as a $\log_{10}$ of the ratio between transfected and control neurons, mean ± s.e.m. ($P > 0.05$, $n = 11$) Black sample traces are control, green traces are transfected cells. Scale bars represent 50 pA and 50 ms.

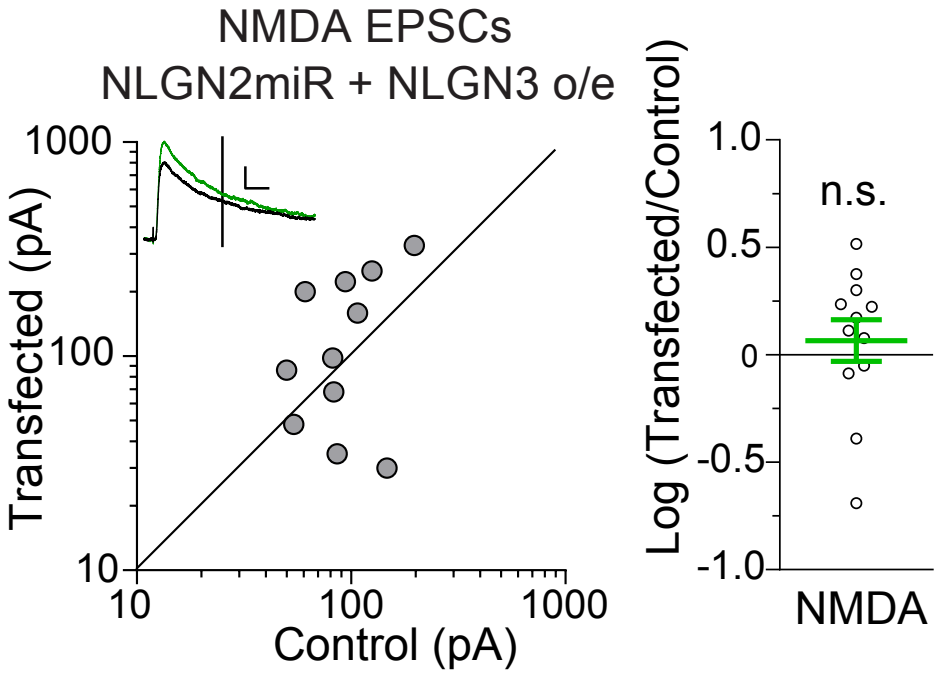
NMDA EPSCs
NLGN2miR + NLGN3 o/e
1000
100
10
Transfected (pA)
10
100
1000
Control (pA)
1.0
0.5
0
-0.5
-1.0
Log (Transfected/Control)
n.s.
NMDA

Figure 5. Model summarizing differences between PV+ and SOM+ synapses.
PV-IPSCs are regulated by sodium channel (Nav) mediated action potentials, a process dependent on L-type calcium channels (LTCC). SOM-IPSCs are regulated by NMDARs, a process dependent on R-type calcium channels (RTCC). PV-IPSCs require neuroligin-2 (NLGN2), while SOM-IPSCs require both NLGN2 and neuroligin-3 (NLGN3). Not pictured are NLGN2/2 or NLGN3/3 homomers, which are also likely present at synapses formed by SOM-expressing inhibitory neurons.

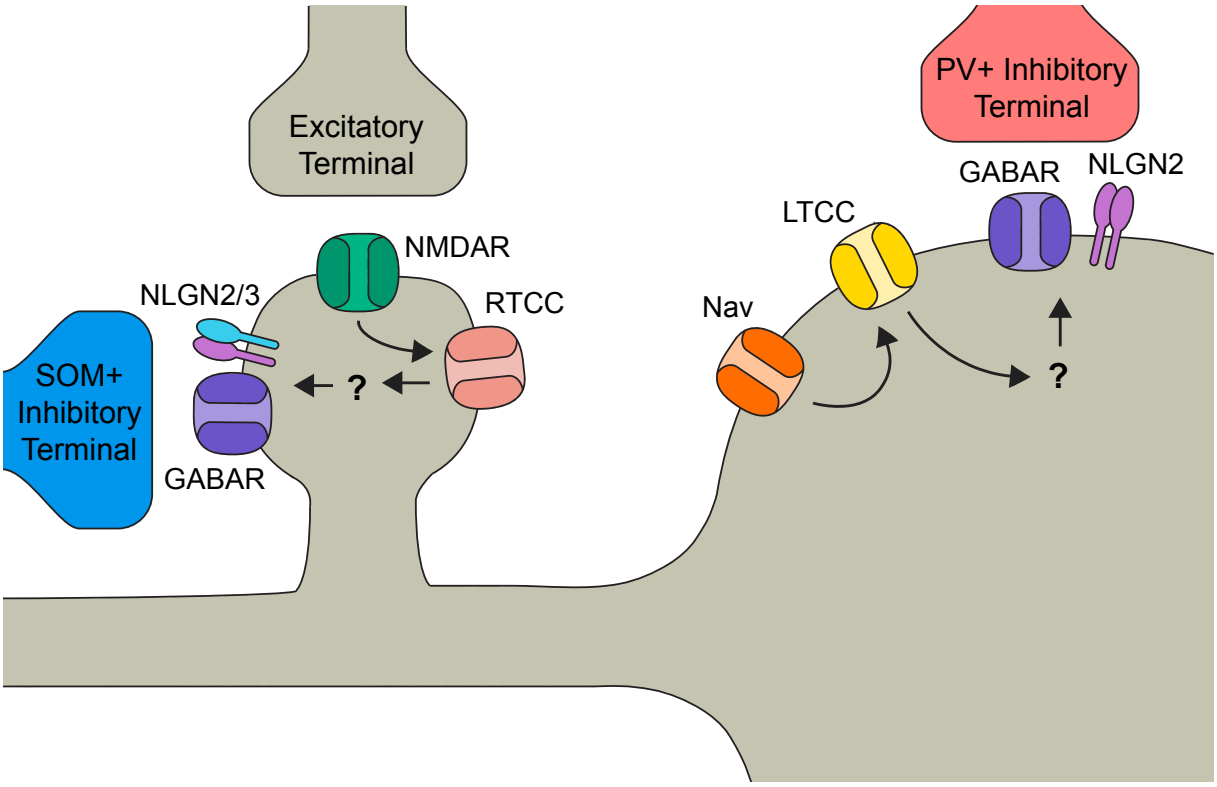
Excitatory Terminal
PV+ Inhibitory Terminal
GABAR
NLGN2
LTCC
NMDAR
NLGN2/3
RTCC
Nav
SOM+ Inhibitory Terminal
?
?
GABAR

CHAPTER 5

General Conclusions

I have shown evidence for a model in which pyramidal neurons can selectively regulate two sets of inhibitory synapses. In Chapter 3, I show that by manipulating different excitatory channels, pyramidal neurons can selectively adjust their PV+ vs. SOM+ input, in a process dependent on different types of voltage-gated calcium channels. In Chapter 4, I found that while several post-synaptic components are shared between PV+ and SOM+ synapses, NLGN3 is capable of selectively and robustly regulating SOM+ synapses. This suggests that there are other proteins specific to SOM+ synapses, which are binding to NLGN3 (discussed further below), and provides evidence that there are indeed molecular differences between synapses formed by different categories of interneurons. Here, I will first discuss the potential caveats in using PV and SOM-Cre mouse lines, then discuss the implications and potential future directions of the results described.

The use of PV and SOM-Cre mouse lines: potential caveats

As discussed in the introduction, PV and SOM-Cre lines label heterogeneous populations (Jiang et al., 2015; Somogyi and Klausberger, 2005). This could be seen as a potential caveat to the interpretation of the results presented here, as it is unclear which of the PV+ or SOM+ subclasses are responsible for the effects shown. However, I propose that the use of these cell-lines is an important first step in studying the molecular mechanisms of GABAergic homeostasis

for three main reasons. (1) PV-expressing cells have already been shown to play a role in action potential-dependent homeostasis (Bartley et al., 2008; Xue et al., 2014). (2) Several reports have demonstrated different functions of PV vs. SOM-expressing interneurons in behavioral paradigms (Funk et al., 2017; Kepecs and Fishell, 2014; Miao et al., 2017; Pinto and Dan, 2015), suggesting that diverging roles for these classes of interneurons might also be found at the cellular level. (3) Despite internal heterogeneity, the majority of PV+ cells are somatic and peri-somatic targeting and the majority of SOM+ cells are dendritic targeting (as discussed more thoroughly in the introduction).

Therefore, if there are different "rules" governing the function of inhibitory synapses depending on the subcellular compartment they target, it should be possible to use PV-Cre and SOM-Cre mice to distinguish them. Given this, we chose to use PV and SOM-Cre mouse lines to further untangle the interneuron subclass specific roles in GABAergic homeostasis, which has traditionally been studied by examining miniature IPSCs (mIPSCs) alone. Now that it does seem that PV+ vs. SOM+ synapses are regulated by different processes, it would be interesting to use the heterogeneity of these lines as an advantage, as discussed in the next section.

Is the "signal" spatial proximity, or intrinsic to the inhibitory synapse?

The results in Chapter 3 point to a model in which there could be different pathways capable of regulating somatic (PV+) vs. dendritic targeting (SOM+) inhibitory neurons. PV-IPSCs are regulated by action potential firing through LTCC, while SOM-IPSCs are regulated by NMDARs through RTCC. It could be that the factor determining which type of synapse is regulated is the proximity of a particular synapse to an excitatory signal (either the action potential initiation site and LTCC for PV-IPSCs, or NMDAR-mediated currents and RTCC for

SOM-IPSCs.) However, another possibility is that there are intrinsic differences between the inhibitory synapses, which govern whether or not they can be regulated by an excitatory signal (either the post-synaptic components or the pre-synaptic terminals). For example, if one could force SOM+ synapses to form at the soma, could they be regulated by action potential firing? While this experiment would be technically unfeasible, as it is unknown which molecular mechanisms underlying targeting patterns, one would be able to use another approach.

One class of PV+ interneurons that targets the dendrites is bistratified neurons. One could perform paired recordings to determine if the unitary PV-IPSCs recorded from ΔNav pyramidal neurons were decreased as compared to unitary PV-IPSCs on untransfected cells. If they were down, it would suggest that there is something intrinsic about the molecular composition of PV+ synapses that makes them susceptible to action potential firing, regardless of which compartment on the cell they target.

It would also be interesting to further parse whether there are particular subcategories of SOM+ cells which are regulated by NMDAR-mediated current. The obvious candidate to begin with would be O-LM neurons, as they represent the largest class of SOM+ cells, and it is possible that it is O-LM alone which are regulated by NMDAR.

Could NLGN3 be downstream of NMDAR dependent SOM-IPSC plasticity?

The results from Chapter 3 show that SOM-IPSCs are selectively regulated by NMDAR-mediated current through RTCCs. In Chapter 4, I found that NLGN3 removal selectively decreases SOM-IPSCs. Could it be that the mechanism through which NMDAR-mediated current regulates SOM-IPSCs is by decreasing NLGN3? While this is certainly a possibility, we there is not yet enough evidence to draw this conclusion.

We have shown that the decrease in SOM-IPSCs in ΔGluN1 cells represents a loss of functional synaptic connections. This could either be due to a decrease in the number of pre-synaptic release sites, or an all-or-none loss of post-synaptic $GABA_AR$-containing clusters. As discussed in Chapter 3, elimination of the post-synaptic scaffolding MAGUK protein family has been shown to cause an all-or-none loss of excitatory synapses, though an LTCC-dependent process termed "consolidation" (Levy et al., 2015). It is therefore theoretically possible that NLGN3 is capable of triggering a similar consolidation of inhibitory synapses, through an RTCC-dependent process. Ideally, one would perform coefficient of variation analysis on SOM-IPSCs from NLGN3 miR cells and determine whether the decrease in currents represents a change in quantal content, similar to the one seen in ΔGluN1 cells. However, coefficient of variation analysis depends upon the using many (ideally over 50), stable (i.e., no signs of "drift" or overall changes in mean peak amplitude from start to finish) traces from each recording session, and there were unfortunately not enough experiments in which I collected the sufficient number of stable traces from the NLGN3 miR and control cells to perform this analysis.

One piece of evidence that NLGN3 is capable of triggering an all-or-none loss of synapses is from the NLGN3 KO mouse. When recording from medium spiny neurons expressing the D1 dopamine receptor, the authors found a decrease in mIPSC frequency but not amplitude (Rothwell et al., 2014). This indicates that the loss of NLGN3 may be decreasing inhibitory synapses in an all-or-none manner. Clearly, more work is needed to determine whether the decrease in SOM-IPSCs in ΔGluN1 cells represents a pre-or post-synaptic change, and then whether NLGN3 may be involved.

Comparison to other forms of NMDAR-dependent inhibitory plasticity

In Chapter 3, I show that SOM-IPSCs are regulated by NMDAR-mediated current in an RTCC-dependent manner. This is not the first study which has found that IPSCs are capable of being regulated by NMDAR-mediated currents. Several reports have previously shown that acute application of NMDA leads to a rapid increase in IPSCs (Marsden et al., 2010, 2007; Petrini et al., 2014), a process termed "inhibitory long term potentiation" (iLTP) due to the rapid increase in IPSCs which recalls excitatory LTP. While these studies did not differentiate between different types of inhibitory input, the results here would suggest that iLTP is mediated by SOM+ synapses. If this were the case, it would mean that there are multiple time scales through which NMDARs can regulate SOM-IPSCs.

In these studies, it was shown that iLTP was dependent on activation of Ca^{2+}/calmodulin-dependent protein kinase II (CaMKII) (Marsden et al., 2010) and gephyrin recruitment (Petrini et al., 2014). It is possible that CaMKII is downstream of the RTCC regulation of SOM-IPSCs presented here, although one study has shown that RTCC activity is not required for basal levels of CaMKII activation, as measured by levels of phospho-T286 (Pasek et al., 2015). An alternative possibility is therefore that the mechanisms governing iLTP differ from those induced by the long-term effects of elimination of NMDAR-mediated current demonstrated here.

The composition of PV+ vs. SOM+ synapses

The experiments in Chapter 4 suggest that many of the components of the iPSD are shared between PV+ and SOM+ synapses. Gephyrin, collybistin, and NLGN2 are necessary to maintain normal levels of both PV and SOM-IPSCs. As discussed in Chapter 4, these results are at odds with a result showing that NLGN2 is not present at SOM+ synapses, potentially due to differences in the techniques used to identify SOM+ neurons and/or brain regions studied. The

results here point towards a model in which gephyrin, collybistin, and NLGN2 all contribute to support inhibitory synapses, though it is unclear whether these proteins are all present at the same group of synapses or whether they can function independently. In the future, it would be interesting to eliminate gephyrin, collybistin, and NLGN2 simultaneously to attempt to completely eliminate all PV and SOM-IPSCs, and determine whether there are some inhibitory synapses capable of forming in the absence of all of these proteins.

The role of NLGN3 at SOM+ synapses

NLGN3 was found to be capable of selectively regulating SOM but not PV-IPSCs (Chapter 4). This leads to the obvious question of what NLGN3 is binding to at these synapses. Extracellularly, NLGN proteins bind to neurexins (NRXN). So if SOM+ interneurons expressed a distinctive NRXN compared to PV+ interneurons, this would be a good candidate to test. Futai et al. (Futai et al., 2013) compared mRNA expression of αNRX1,2,3 and βNRX1,2,3 in both CA3 pyramidal neurons as well as SOM+, CCK+, and PV+ interneurons. However, the authors only reported significant increases of αNRXN1 and βNRXN1 in pyramidal neurons compared to all interneurons (Futai et al., 2013). It appears that there are slightly higher levels of αNRXN1 in SOM+ and CCK+ neurons, compared to PV+ inhibitory neurons, making αNRXN1 the a good candidate to test further with higher numbers of cells (less than 10 cells per group were used in this study). NLGN3 has also been shown to induce clustering of gephyrin in COS cells when co-cultured with neurons overexpressing βNRXN1 (either with or without an insertion at splice site 4) (Budreck and Scheiffele, 2007), providing another possibility for a binding partner. Unfortunately, other isoforms of NRXN were not tested in this study.

Intracellularly, NLGN3 contains binding domains for both gephyrin and a PDZ-binding domain (Nguyen et al., 2016). As knocking down gephyrin leads to a decrease in both PV and SOM-IPSCs (Chapter 2), it is unclear how this protein would control SOM+ synapse specific effects. It is also not known which PDZ-domain containing proteins would function at inhibitory synapses.

A study in the retina in the NLGN3 KO mouse showed fewer $GABA_AR$ α2 containing puncta than wild-type retina tissues, while gephyrin, $GABA_AR$ α1, γ2, and PSD-95 puncta remained unaltered. However, it is unlikely $GABA_AR$ α2 is exclusively localized to SOM+ synapses, as it has also been shown to localize to the axon initial segment (Panzanelli et al., 2011) as well as certain synapses at the soma (Nyíri et al., 2001). Nevertheless, Panzanelli et al. also found a high cluster density of puncta containing $GABA_AR$ α2, NLGN2, and gephyrin in stratum lacunosum moleculare, which persisted in the $GABA_AR$ α2 KO (Panzanelli et al., 2011). This suggests that these three proteins, along with another capable of stabilizing inhibitory synapses in the absence of $GABA_AR$ α2, may be supporting SOM+ synapses.

Possibility of different secretory pathways for PV and SOM synapses

While the focus of the work shown here was to examine proteins known to regulate the surface trafficking of $GABA_AR$, an intriguing alternative possibility is pyramidal neurons may be differentially regulating sets of synapses through secretory pathway. Several proteins have been identified in regulating $GABA_AR$-containing vesicles as they are trafficked through each step of the secretory pathway, including from endoplasmic reticulum to the Golgi network, from the Golgi network to the plasma membrane, as well as recycling, endosomal transport pathways (Luscher et al., 2011).

Of particular interest is $GABA_AR$ associated protein (GABARAP). First pulled down in a yeast two-hyrbid screen using the $GABA_AR$ γ2 subunit as bait (Wang et al., 1999), GABARAP is thought to interact with both $GABA_AR$ and N-ethylmaleimide sensitive factor, a protein critical for vesicle fusion, and enriched in the *trans*-Golgi network (Luscher et al., 2011). Relevant to the work presented here, while acute NMDA application normally causes an increase in surface expression of $GABA_AR$ β2/3 subunits, knock-down of GABARAP prevents this from occurring (Marsden et al., 2007). Therefore, if it is specifically the SOM-IPSCs which are regulated by NMDA application, GABARAP may be a good candidate for a protein which is involved in delivering vesicles containing $GABA_AR$ from the Golgi network to SOM+ synapses. There is also evidence that chronic activity blockade with TTX causes an increase in $GABA_AR$ ubiquitination (Saliba et al., 2007), suggesting that the proteasomal degradation pathway may also be involved in the homeostatic pathways described here.

The End Game: Just keep splitting?

In 2016, we (Nguyen et al., 2016) published a study investigating the role of NLGN3 at inhibitory synapses, recording IPSCs induced with a bipolar electrode placed in CA1. Transfecting neurons with NLGN3 miR caused no significant change in IPSCs, and overexpression of NLGN3 caused no increase of IPSCs when performed on a NLGN2 miR background. As NLGN3 expressed without the NLGN2 miR did cause an increase in IPSCs, we interpreted these results to mean that NLGN3 could only affect inhibitory synapses when it's able to heterodimerize with NLGN2.

In light of the results presented in Chapter 4, we now must revise our interpretation of this data. While it appeared that the NLGN3 miR had no effect on inhibitory synapses, it appears

that the effects might have been masked by the use of electrically-induced IPSCs, as we now know that SOM-IPSCs are decreased, and PV-IPSCs are slightly (though not significantly) increased. And while it appeared that overexpressing NLGN3 on a NLGN2 miR background had no effect on IPSCs, it is now clear that the dramatic enhancement of SOM-IPSCs, combined with a severe reduction of PV-IPSCs would also give the appearance of there being no significant effects on electrically-induced IPSCs. Another lab has since published the finding that reduction of NLGN3 has no effect on electrically-induced IPSCs onto pyramidal neurons in the hippocampus (Chanda et al., 2017). The authors of that study conclude that NLGN3 "has no significant essential effect" at inhibitory synapses.

The results presented here suggest that any study using electrically-induced IPSCs to conclude that a manipulation has no effect on inhibitory synapses cannot rule out the possibility that the same manipulation might be exerting dramatic but opposing effects on interneuron subtype specific synapses.

Many might argue that using PV and SOM-Cre lines is *still* activating too heterogeneous a population to make any conclusions. For the goal of systematically categorizing the possible sub-type specific effects every synaptic protein or plasticity pathway, it is indeed imperative that we find efficient ways of genetically targeting each of the ~20 subtypes of inhibitory neurons. However, perhaps it is possible to use the tools already at our disposal to determine some candidate principles underlying the regulation of inhibitory transmission onto subcellular compartments of principal neurons.

References

Alger, B.E., Pitler, T.A., 1995. Retrograde signaling at GABAA-receptor synapses in the mammalian CNS. Trends Neurosci. 18, 333–340.

Atallah, B. V., Scanziani, M., 2009. Instantaneous Modulation of Gamma Oscillation Frequency by Balancing Excitation with Inhibition. Neuron 62, 566–577.

Bartley, A.F., Huang, Z.J., Huber, K.M., Gibson, J.R., 2008. Differential activity-dependent, homeostatic plasticity of two neocortical inhibitory circuits. J. Neurophysiol. 100, 1983–1994.

Bezaire, M.J., Soltesz, I., 2013. Quantitative assessment of CA1 local circuits: Knowledge base for interneuron-pyramidal cell connectivity. Hippocampus 23, 751–785.

Blasco-Ibáñez, J.M., Freund, T.F., 1995. Synaptic Input of Horizontal Interneurons in Stratum Oriens of the Hippocampal CA1 Subfield: Structural Basis of Feed-back Activation. Eur. J. Neurosci. 7, 2170–2180. doi:10.1111/j.1460-9568.1995.tb00638.x

Budreck, E.C., Scheiffele, P., 2007. Neuroligin-3 is a neuronal adhesion protein at GABAergic and glutamatergic synapses. Eur. J. Neurosci. 26, 1738–1748.

Chanda, S., Hale, W.D., Zhang, B., Wernig, M., Südhof, T.C., 2017. Unique versus Redundant Functions of Neuroligin Genes in Shaping Excitatory and Inhibitory Synapse Properties. J. Neurosci. 37, 6816–6836.

Davare, M.A., Avdonin, V., Hall, D.D., Peden, E.M., Burette, A., Weinberg, R.J., Horne, M.C., Hoshi, T., Hell, J.W., 2001. A β2 Adrenergic Receptor Signaling Complex Assembled with the Ca2+ Channel Cav1.2. Science (80-.). 293, 98–101.

Di Cristo, G., Wu, C., Chattopadhyaya, B., Ango, F., Knott, G., Welker, E., Svoboda, K., Huang, Z.J., 2004. Subcellular domain-restricted GABAergic innervation in primary visual cortex in the absence of sensory and thalamic inputs. Nat. Neurosci. 7, 1184–6.

Eichler, S.A., 2008. E-I balance and human diseases – from molecules to networking. Front. Mol. Neurosci. 1, 1–5. doi:10.3389/neuro.02.002.2008

Fairén, A., 2007. Cajal and Lorente de Nó on cortical interneurons: Coincidences and progress. Brain Res. Rev. 55, 430–444. doi:10.1016/j.brainresrev.2007.06.004

Felts, P.A., Yokoyama, S., Dib-Hajj, S., Black, J.A., Waxman, S.G., 1997. Sodium channel alpha-subunit mRNAs I, II, III, NaG, Na6 and hNE (PN1): different expression patterns in developing rat nervous system. Brain Res. Mol. Brain Res. 45, 71–82.

Földy, C., Malenka, R.C., Südhof, T.C., 2013. Autism-associated neuroligin-3 mutations commonly disrupt tonic endocannabinoid signaling. Neuron 78, 498–509.

Früh, S., Romanos, J., Panzanelli, P., Bürgisser, D., Tyagarajan, S.K., Campbell, K.P., Santello, M., Fritschy, J.-M., 2016. Neuronal Dystroglycan Is Necessary for Formation and Maintenance of Functional CCK-Positive Basket Cell Terminals on Pyramidal Cells. J. Neurosci. 36, 10296–10313. doi:10.1523/JNEUROSCI.1823-16.2016

Funk, C.M., Peelman, K., Bellesi, M., Marshall, W., Cirelli, C., Tononi, G., 2017. Role of somatostatin-positive cortical interneurons in the generation of sleep slow waves. J. Neurosci. 37, 1303–17. doi:10.1523/JNEUROSCI.1303-17.2017

Futai, K., Doty, C.D., Baek, B., Ryu, J., Sheng, M., 2013. Specific Trans-Synaptic Interaction with Inhibitory Interneuronal Neurexin Underlies Differential Ability of Neuroligins to Induce Functional Inhibitory Synapses. J. Neurosci. 33, 3612–3623. doi:10.1523/JNEUROSCI.1811-12.2013

Gao, R., Penzes, P., 2015. Common mechanisms of excitatory and inhibitory imbalance in schizophrenia and autism spectrum disorders. Curr. Mol. Med. 15, 146–67.

Gibson, J.R., Huber, K.M., Sudhof, T.C., 2009. Neuroligin-2 Deletion Selectively Decreases Inhibitory Synaptic Transmission Originating from Fast-Spiking but Not from Somatostatin-Positive Interneurons. J. Neurosci. 29, 13883–13897.

Goold, C.P., Nicoll, R.A., 2010. Single-Cell Optogenetic Excitation Drives Homeostatic Synaptic Depression. Neuron 68, 512–528.

Gray, J.A., Shi, Y., Usui, H., During, M.J., Sakimura, K., Nicoll, R.A., 2011. Article Distinct Modes of AMPA Receptor Suppression at Developing Synapses by GluN2A and GluN2B : Single-Cell NMDA Receptor Subunit Deletion In Vivo. Neuron 71, 1085–1101.

Gu, X., Zhou, L., Lu, W., 2016. An NMDA Receptor-Dependent Mechanism Underlies Inhibitory Synapse Development. Cell Rep. 14, 471–478.

Haider, B., Duque, A., Hasenstaub, A.R., McCormick, D.A., 2006. Neocortical network activity in vivo is generated through a dynamic balance of excitation and inhibition. J. Neurosci. 26, 4535–45.

Hartman, K.N., Pal, S.K., Burrone, J., Murthy, V.N., 2006. Activity-dependent regulation of inhibitory synaptic transmission in hippocampal neurons. Nat. Neurosci. 9, 642–649.

Hu, H., Gan, J., Jonas, P., 2014. Fast-spiking, parvalbumin+ GABAergic interneurons: From cellular design to microcircuit function. Science (80-.). 345, 1255263–1255263. doi:10.1126/science.1255263

Ibata, K., Sun, Q., Turrigiano, G.G., 2008. Rapid Synaptic Scaling Induced by Changes in Postsynaptic Firing. Neuron 57, 819–826.

Incontro, S., Asensio, C.S., Edwards, R.H., Nicoll, R.A., 2014. Efficient, Complete Deletion of

Synaptic Proteins using CRISPR. Neuron 83, 1051–1057.

Jacob, T.C., Bogdanov, Y.D., Magnus, C., Saliba, R.S., Kittler, J.T., Haydon, P.G., Moss, S.J., 2005. Gephyrin regulates the cell surface dynamics of synaptic GABAA receptors. J. Neurosci. 25, 10469–78. doi:10.1523/JNEUROSCI.2267-05.2005

Jacob, T.C., Moss, S.J., Jurd, R., 2008. GABAA receptor trafficking and its role in the dynamic modulation of neuronal inhibition. Nat. Rev. Neurosci. 9, 331–343. doi:10.1038/nrn2370

Jiang, X., Shen, S., Cadwell, C.R., Berens, P., Sinz, F., Ecker, A.S., Patel, S., Tolias, A.S., 2015. Principles of connectivity among morphologically defined cell types in adult neocortex. Science 350, aac9462.

Kang, Y., Ge, Y., Cassidy, R.M., Lam, V., Luo, L., Moon, K.M., Lewis, R., Molday, R.S., Wong, R.O.L., Foster, L.J., Craig, A.M., 2014. A combined transgenic proteomic analysis and regulated trafficking of neuroligin-2. J. Biol. Chem. 289, 29350–29364. doi:10.1074/jbc.M114.549279

Kepecs, A., Fishell, G., 2014. Interneuron cell types are fit to function. Nature 505, 318–26.

Kilman, V., van Rossum, M.C.W., Turrigiano, G.G., 2002. Activity deprivation reduces miniature IPSC amplitude by decreasing the number of postsynaptic GABA(A) receptors clustered at neocortical synapses. J. Neurosci. 22, 1328–1337. doi:22/4/1328 [pii]

Kins, S., Betz, H., Kirsch, J., 2000. Collybistin, a newly identified brain-specific GEF, induces submembrane clustering of gephyrin. Nat. Neurosci. 3, 22–29. doi:10.1038/71096

Klausberger, T., Roberts, J.D.B., Somogyi, P., 2002. Cell type- and input-specific differences in the number and subtypes of synaptic GABA(A) receptors in the hippocampus. J. Neurosci. 22, 2513–21. doi:20026228

Klausberger, T., Somogyi, P., 2008. Neuronal Diversity and Temporal Dynamics: The Unity of Hippocampal Circuit Operations. Science (80-.). 321, 53–57. doi:10.1126/science.1149381

Kneussel, M., Helmut Brandstätter, J., Gasnier, B., Feng, G., Sanes, J.R., Betz, H., 2001. Gephyrin-Independent Clustering of Postsynaptic GABAA Receptor Subtypes. Mol. Cell. Neurosci. 17, 973–982. doi:10.1006/mcne.2001.0983

Knuesel, I., Mastrocola, M., Zuellig, R.A., Bornhauser, B., Schaub, M.C., Fritschy, J.-M., 1999. Altered synaptic clustering of GABA $_A$ receptors in mice lacking dystrophin (mdx mice). Eur. J. Neurosci. 11, 4457–4462. doi:10.1046/j.1460-9568.1999.00887.x

Körber, C., Richter, A., Kaiser, M., Schlicksupp, A., Mükusch, S., Kuner, T., Kirsch, J., Kuhse, J., 2012. Effects of distinct collybistin isoforms on the formation of GABAergic synapses in hippocampal neurons. Mol. Cell. Neurosci. 50, 250–259. doi:10.1016/j.mcn.2012.05.006

Kuhse, J., Kalbouneh, H., Schlicksupp, A., Mükusch, S., Nawrotzki, R., Kirsch, J., 2012. Phosphorylation of gephyrin in hippocampal neurons by cyclin-dependent kinase CDK5 at Ser-270 is dependent on collybistin. J. Biol. Chem. 287, 30952–30966. doi:10.1074/jbc.M112.349597

Kurotani, T., Yamada, K., Yoshimura, Y., Crair, M.C., Komatsu, Y., 2008. State-Dependent Bidirectional Modification of Somatic Inhibition in Neocortical Pyramidal Cells. Neuron 57, 905–916.

Lévi, S., Logan, S.M., Tovar, K.R., Craig, A.M., 2004. Gephyrin Is Critical for Glycine Receptor Clustering But Not for the Formation of Functional GABAergic Synapses in Hippocampal Neurons. J. Neurosci. 24, 207 LP-217.

Levy, J.M., Chen, X., Reese, T.S., Nicoll, R.A., 2015. Synaptic Consolidation Normalizes AMPAR Quantal Size following MAGUK Loss. Neuron 87, 534–548.

Lu, W., Bushong, E.A., Shih, T.P., Ellisman, M.H., Nicoll, R.A., 2013. The cell-autonomous role of excitatory synaptic transmission in the regulation of neuronal structure and function. Neuron 78, 433–439.

Luscher, B., Fuchs, T., Kilpatrick, C.L., 2011. GABAA Receptor Trafficking-Mediated Plasticity of Inhibitory Synapses. Neuron 70, 385–409. doi:10.1016/j.neuron.2011.03.024

Marsden, K.C., Beattie, J.B., Friedenthal, J., Carroll, R.C., 2007. NMDA Receptor Activation Potentiates Inhibitory Transmission through GABA Receptor-Associated Protein-Dependent Exocytosis of GABA A Receptors. J. Neurosci. 27, 14326–14337.

Marsden, K.C., Shemesh, A., Bayer, K.U., Carroll, R.C., 2010. Selective translocation of Ca2+/calmodulin protein kinase IIalpha (CaMKIIalpha) to inhibitory synapses. Proc. Natl. Acad. Sci. U. S. A. 107, 20559–20564.

Miao, C., Cao, Q., Moser, M.B., Moser, E.I., 2017. Parvalbumin and Somatostatin Interneurons Control Different Space-Coding Networks in the Medial Entorhinal Cortex. Cell 171, 507–509.e17. doi:10.1016/j.cell.2017.08.050

Nguyen, Q.A., Horn, M.E., Nicoll, R.A., 2016. Distinct roles for extracellular and intracellular domains in neuroligin function at inhibitory synapses. Elife 5, 1–21.

Nugent, F.S., Penick, E.C., Kauer, J. a, 2007. Opioids block long-term potentiation of inhibitory synapses. Nature 446, 1086–90.

Nyíri, G., Freund, T.F., Somogyi, P., 2001. Input-dependent synaptic targeting of alpha(2)-subunit-containing GABA(A) receptors in synapses of hippocampal pyramidal cells of the rat. Eur. J. Neurosci. 13, 428–442. doi:10.1046/j.1460-9568.2001.01407.x

Okun, M., Lampl, I., 2008. Instantaneous correlation of excitation and inhibition during ongoing

and sensory-evoked activities. Nat. Neurosci. 11, 535–7.

Panzanelli, P., Gunn, B.G., Schlatter, M.C., Benke, D., Tyagarajan, S.K., Scheiffele, P., Belelli, D., Lambert, J.J., Rudolph, U., Fritschy, J.-M., 2011. Distinct mechanisms regulate GABAA receptor and gephyrin clustering at perisomatic and axo-axonic synapses on CA1 pyramidal cells. J. Physiol. 589, 4959–80. doi:10.1113/jphysiol.2011.216028

Papadopoulos, T., Korte, M., Eulenburg, V., Kubota, H., Retiounskaia, M., Harvey, R.J., Harvey, K., O'Sullivan, G.A., Laube, B., Hülsmann, S., Geiger, J.R.P., Betz, H., 2007. Impaired GABAergic transmission and altered hippocampal synaptic plasticity in collybistin-deficient mice. EMBO J. 26, 3888–3899. doi:10.1038/sj.emboj.7601819

Pasek, J.G., Wang, X., Colbran, R.J., 2015. Differential CaMKII regulation by voltage-gated calcium channels in the striatum. Mol. Cell. Neurosci. 68, 234–243. doi:10.1016/j.mcn.2015.08.003

Peng, Y.-R., Zeng, S.-Y., Song, H.-L., Li, M.-Y., Yamada, M.K., Yu, X., 2010. Postsynaptic spiking homeostatically induces cell-autonomous regulation of inhibitory inputs via retrograde signaling. J. Neurosci. 30, 16220–16231.

Petrini, E.M., Ravasenga, T., Hausrat, T.J., Iurilli, G., Olcese, U., Racine, V., Sibarita, J.-B., Jacob, T.C., Moss, S.J., Benfenati, F., Medini, P., Kneussel, M., Barberis, A., 2014. Synaptic recruitment of gephyrin regulates surface GABAA receptor dynamics for the expression of inhibitory LTP. Nat. Commun. 5, 3921.

Pinto, L., Dan, Y., 2015. Cell-Type-Specific Activity in Prefrontal Cortex during Goal-Directed Behavior. Neuron 87, 437–451. doi:10.1016/j.neuron.2015.06.021

Pouille, F., Scanziani, M., 2001. Enforcement of Temporal Fidelity in Pyramidal Cells by Somatic Feed-Forward Inhibition. Science (80-.). 293, 1159 LP-1163.

Poulopoulos, A., Aramuni, G., Meyer, G., Soykan, T., Hoon, M., Papadopoulos, T., Zhang, M., Paarmann, I., Fuchs, C., Harvey, K., Jedlicka, P., Schwarzacher, S.W., Betz, H., Harvey, R.J., Brose, N., Zhang, W., Varoqueaux, F., 2009. Neuroligin 2 Drives Postsynaptic Assembly at Perisomatic Inhibitory Synapses through Gephyrin and Collybistin. Neuron 63, 628–642. doi:10.1016/j.neuron.2009.08.023

Pribiag, H., Peng, H., Shah, W.A., Stellwagen, D., Carbonetto, S., 2014. Dystroglycan mediates homeostatic synaptic plasticity at GABAergic synapses. Proc. Natl. Acad. Sci. 111, 6810–6815. doi:10.1073/pnas.1321774111

Qiao, X., Werkman, T.R., Gorter, J.A., Wadman, W.J., van Vliet, E.A., 2013. Expression of sodium channel alpha subunits 1.1, 1.2 and 1.6 in rat hippocampus after kainic acid-induced epilepsy. Epilepsy Res. 106, 17–28.

Rothwell, P.E., Fuccillo, M. V., Maxeiner, S., Hayton, S.J., Gokce, O., Lim, B.K., Fowler, S.C.,

Malenka, R.C., Südhof, T.C., 2014. Autism-associated neuroligin-3 mutations commonly impair striatal circuits to boost repetitive behaviors. Cell 158, 198–212. doi:10.1016/j.cell.2014.04.045

Rutherford, L.C., DeWan, A., Lauer, H.M., Turrigiano, G.G., 1997. Brain-derived neurotrophic factor mediates the activity-dependent regulation of inhibition in neocortical cultures. J. Neurosci. 17, 4527–4535.

Sakurada, K., Masu, M., Nakanishi, S., 1993. Alteration of Ca2+ permeability and sensitivity to Mg2+ and channel blockers by a single amino acid substitution in the N-methyl-D-aspartate receptor. J. Biol. Chem. 268, 410–415.

Saliba, R.S., Michels, G., Jacob, T.C., Pangalos, M.N., Moss, S.J., 2007. Activity-Dependent Ubiquitination of GABAA Receptors Regulates Their Accumulation at Synaptic Sites. J. Neurosci. 27, 13341–13351. doi:10.1523/JNEUROSCI.3277-07.2007

Schlick, B., Flucher, B.E., Obermair, G.J., 2010. Voltage-activated calcium channel expression profiles in mouse brain and cultured hippocampal neurons. Neuroscience 167, 786–798.

Schnell, E., Sizemore, M., Karimzadegan, S., Chen, L., Bredt, D.S., Nicoll, R.A., 2002. Direct interactions between PSD-95 and stargazin control synaptic AMPA receptor number. Proc. Natl. Acad. Sci. U. S. A. 99, 13902–7. doi:10.1073/pnas.172511199

Shipman, S.L., Nicoll, R.A., 2012. A Subtype-Specific Function for the Extracellular Domain of Neuroligin 1 in Hippocampal LTP. Neuron 76, 309–316. doi:10.1016/j.neuron.2012.07.024

Shipman, S.L., Schnell, E., Hirai, T., Chen, B., Roche, K.W., Nicoll, R.A., 2011. Functional dependence of neuroligin on a new non-PDZ intracellular domain. Nat. Neurosci. 14, 718–726.

Somogyi, P., Klausberger, T., 2005. Defined types of cortical interneurone structure space and spike timing in the hippocampus. J. Physiol. 562, 9–26.

Stoppini, L., Buchs, P.A., Muller, D., 1991. A simple method for organotypic cultures of nervous tissue. J. Neurosci. Methods 37, 173–82.

Straub, C., Granger, A.J., Saulnier, J.L., Sabatini, B.L., 2014. CRISPR/Cas9-mediated gene knock-down in post-mitotic neurons. PLoS One 9, 1–5.

Südhof, T.C., 2017. Synaptic Neurexin Complexes: A Molecular Code for the Logic of Neural Circuits. Cell 171, 745–769. doi:10.1016/j.cell.2017.10.024

Swanwick, C.C., Murthy, N.R., Kapur, J., 2006. Activity-dependent scaling of GABAergic synapse strength is regulated by brain-derived neurotrophic factor. Mol. Cell. Neurosci. 31, 481–492. doi:10.1016/j.mcn.2005.11.002

Tabuchi, K., Blundell, J., Etherton, M.R., Hammer, R.E., Liu, X., Powell, C.M., Sudhof, T.C., 2007. A Neuroligin-3 Mutation Implicated in Autism Increases Inhibitory Synaptic Transmission in Mice. Science (80-.). 318, 71–76. doi:10.1126/science.1146221

Thiagarajan, T.C., Lindskog, M., Tsien, R.W., 2005. Adaptation to synaptic inactivity in hippocampal neurons. Neuron 47, 725–737.

Thomson, A.M., Bannister, A.P., Hughes, D.I., Pawelzik, H., 2000. Differential sensitivity to Zolpidem of IPSPs activated by morphologically identified CA1 interneurons in slices of rat hippocampus. Eur. J. Neurosci. 12, 425–436. doi:10.1046/j.1460-9568.2000.00915.x

Tremblay, R., Lee, S., Rudy, B., 2016. GABAergic Interneurons in the Neocortex: From Cellular Properties to Circuits. Neuron 91, 260–292.

Turrigiano, G., 2011. Stabilizing Neuronal Function Homeostatic Synaptic Plasticity: Local and Global Mechanisms for Homeostatic Synaptic Plasticity: Local and Global Mechanisms for Stabilizing Neuronal Function. Cold Spring Harb Perspect Biol 1–18. doi:10.1101/cshperspect.a005736

Turrigiano, G.G., Leslie, K.R., Desai, N.S., Rutherford, L.C., Nelson, S.B., 1998. Activity-dependent scaling of quantal amplitude in neocortical neurons. Nature 391, 892–896. doi:10.1038/36103

Uezu, A., Kanak, D.J., Bradshaw, T.W.A., Soderblom, E.J., Catavero, C.M., Burette, A.C., Weinberg, R.J., Soderling, S.H., 2016. Identification of an elaborate complex mediating postsynaptic inhibition. Science (80-.). 353, 1123–1129.

Varoqueaux, F., Jamain, S., Brose, N., 2004. Neuroligin 2 is exclusively localized to inhibitory synapses. Eur. J. Cell Biol. 83, 449–456.

Villa, K.L., Berry, K.P., Subramanian, J., Cha, J.W., Oh, W.C., Kwon, H.B., Kubota, Y., So, P.T.C., Nedivi, E., 2016. Inhibitory Synapses Are Repeatedly Assembled and Removed at Persistent Sites In Vivo. Neuron 89, 756–769.

Wang, H., Bedford, F.K., Brandon, N.J., Moss, S.J., Olsen, R.W., 1999. GABA(A)-receptor-associated protein links GABA(A) receptors and the cytoskeleton. Nature 397, 69–72. doi:10.1038/16264

Wehr, M.S., Zador, A.M., 2003. Balanced inhibition underlies tuning and sharpens spike timing in auditory cortex. Nature 426, 442–6.

Wilent, W.B., Contreras, D., 2004. Synaptic responses to whisker deflections in rat barrel cortex as a function of cortical layer and stimulus intensity. J Neurosci 24, 3985–3998.

Wilson, R.I., Kunos, G., Nicoll, R.A., 2001. Presynaptic specificity of endocannabinoid signaling in the hippocampus. Neuron 31, 453–462. doi:10.1016/S0896-6273(01)00372-5

Wilson, R.I., Nicoll, R.A., 2001. Endogenous cannabinoids mediate retrograde signalling at hippocampal synapses. Nature 410, 588–592. doi:10.1038/35069076

Xue, M., Atallah, B. V, Scanziani, M., 2014. Equalizing excitation-inhibition ratios across visual cortical neurons. Nature 511, 596–600.

Yasuda, R., Sabatini, B.L., Svoboda, K., 2003. Plasticity of calcium channels in dendritic spines. Nat. Neurosci. 6, 948–55.

Publishing Agreement

It is the policy of the University to encourage the distribution of all theses, dissertations, and manuscripts. Copies of all UCSF theses, dissertations, and manuscripts will be routed to the library via the Graduate Division. The library will make all theses, dissertations, and manuscripts accessible to the public and will preserve these to the best of their abilities, in perpetuity.

I hereby grant permission to the Graduate Division of the University of California, San Francisco to release copies of my thesis, dissertation, or manuscript to the Campus Library to provide access and preservation, in whole or in part, in perpetuity.

Author Signature  Date 12/19/17